Real time response on dS_3: the topological AdS black hole and the bubble

JHEP04(2009)063

(http://iopscience.iop.org/1126-6708/2009/04/063)

Published by IOP Publishing for SISSA

Received: *March 2, 2009*
Accepted: *March 31, 2009*
Published: *April 16, 2009*

Real time response on dS_3: the topological AdS black hole and the bubble

Jimmy A. Hutasoit,[a] **S. Prem Kumar**[b] **and James Rafferty**[b]

[a] *Department of Physics, Carnegie Mellon University, Pittsburgh, PA15213, U.S.A.*
[b] *Department of Physics, Swansea University, Singleton Park, Swansea, SA2 8PP, U.K.*
E-mail: jhutasoi@andrew.cmu.edu, s.p.kumar@swansea.ac.uk, pyjames@swansea.ac.uk

Abstract: We study real time correlators in strongly coupled $\mathcal{N} = 4$ supersymmetric Yang-Mills theory on $dS_3 \times S^1$, with antiperiodic boundary conditions for fermions on the circle. When the circle radius is larger than a critical value, the dual geometry is the so-called "topological AdS_5 black hole". Applying the Son-Starinets recipe in this background we compute retarded glueball propagators which exhibit an infinite set of poles yielding the quasinormal frequencies of the topological black hole. The imaginary parts of the propagators exhibit thermal effects associated with the Gibbons-Hawking temperature due to the cosmological horizon of the de Sitter boundary. We also obtain R-current correlators and find that after accounting for a small subtlety, the Son-Starinets prescription yields the retarded Green's functions. The correlators do not display diffusive behaviour at late times. Below the critical value of the circle radius, the topological black hole decays to the AdS_5 "bubble of nothing". Using a high frequency WKB approximation, we show that glueball correlators in this phase exhibit poles on the real axis. The tunnelling from the black hole to the bubble is interpreted as a hadronization transition.

Keywords: Gauge-gravity correspondence, AdS-CFT Correspondence

ArXiv ePrint: 0902.1658

doi:10.1088/1126-6708/2009/04/063

JHEP04(2009)063

Contents

1 Introduction

Time dependent backgrounds in gravity and in string theory are of great interest from the standpoint of the AdS/CFT correspondence [1, 2] and related holographic dualities between gauge theories and gravity. Time dependent classical gravity backgrounds, in asymptotically Anti-de-Sitter spacetimes, can potentially provide a fully nonperturbative description of non-equilibrium phenomena in the strongly coupled dual gauge theories. Such non-equilibrium physics in field theories arises, most notably, in cosmology and in heavy ion collisions at RHIC. To understand how gauge/gravity dualities work for such

JHEP04(2009)063

processes, it is important to investigate how holography applies in various examples with explicit time dependence. In this paper we attempt the holographic computation of real time correlators of the boundary gauge theory dual to the time dependent, asymptotically *locally* AdS backgrounds found in [3–7].

The authors of [8] studied the double analytic continuations of vacuum solutions such as Schwarzschild and Kerr spacetimes providing examples of smooth, time dependent solutions called "bubbles of nothing" [9–11]. These asymptotically flat solutions were generalized to asymptotically locally AdS spacetimes in [3, 4], by considering the double analytic continuations of AdS black holes.[1] The bubbles are obtained by analytically continuing the time coordinate to Euclidean signature $t \to i\chi$ where χ is periodically identified, and a polar angle $\theta \to i\tau$. In addition, the χ circle has supersymmetry breaking boundary conditions for fermions. The resulting "bubbles" undergo exponential de Sitter expansion (and contraction). For the asymptotically locally $AdS_5 \times S^5$ case [4], the conformal boundary of the geometry is $dS_3 \times S^1$. The corresponding dual field theory, $\mathcal{N} = 4$ SYM, is thus formulated on $dS_3 \times S^1$ with antiperiodic boundary conditions for the fermions around S^1. Each of the two AdS-Schwarzschild black holes (the small and big black holes) yield an AdS bubble of nothing solution, only one of which is stable. The bubble of nothing geometries are vacuum solutions with cosmological horizons [8] and particle creation effects.

It was realized in [5–7] that there is another spacetime with the same AdS asymptotics as the bubble geometries, with $dS_3 \times S^1$ conformal boundary. This is the so-called "topological black hole"[2] – a quotient of AdS space obtained by an identification of global AdS_5 along a boost [17, 18]. It is the five dimensional analog of the BTZ black hole [19, 20]. The topological AdS black hole can also be obtained by a Wick rotation of thermal AdS space. As Euclidean thermal AdS space can be unstable to decay to the big AdS black hole via the first order Hawking-Page transition [21, 22], a similar instability is associated to the topological AdS black hole. In this case the topological AdS black hole is unstable to semiclassical decay via the nucleation of an AdS bubble of nothing. The associated bounce solution is the Euclidean small AdS-Schwarzschild black hole which has a non-conformal negative mode. The topological black hole becomes unstable only when the radius of the spatial circle becomes smaller than a critical value (in the Euclidean thermal setup this is when the temperature exceeds a critical value). Precisely such an instability to decay to "nothing" was, of course, first noted for flat space times a circle having antiperiodic boundary conditions for fermions [9].

The two different geometries described above are dual to two different phases of strongly coupled, large N gauge theory formulated on $dS_3 \times S^1$. As in the usual thermal interpretation wherein the field theory lives on $S^3 \times S^1$, the two phases are distinguished by the expectation value of the Wilson loop around the S^1. In the bubble of nothing phase, the circle shrinks to zero size in the interior of the geometry and the Wilson loop is non-zero, indicating the spontaneous breaking of the $\mathbb{Z}_N$ symmetry of the gauge theory. The

[1] For the classifications of solutions obtained by analytically continuing black hole solutions, see [12].

[2] The term "topological AdS black hole" has also been used to refer to black holes with a hyperbolic horizon having a non-trivial topology. In the AdS/CFT context these have been studied in [13–16] and references therein.

JHEP04(2009)063

topological black hole phase is $\mathbb{Z}_N$ invariant. Unlike the thermal situation however, the spontaneous breaking of $\mathbb{Z}_N$ invariance is not a deconfinement transition since the circle is a spatial direction and not the thermal circle.

Our primary motivation in this article is to understand how the behaviour of real time correlators in the two geometries reflects the properties and distinguishes the two phases of the $\mathcal{N} = 4$ theory on $dS_3 \times S^1$. Since the de Sitter boundary has its own cosmological horizon accompanied by a Gibbons-Hawking radiation [23], this should also be reflected in the properties of the boundary correlation functions. An interesting feature of both the geometries in question is that infinity is connected, i.e. the asymptotics is unlike the (AdS-)Schwarzschild black hole whose asymptotics consists of two disconnected boundaries. This means the Schwinger-Keldysh approach in [24] is not directly applicable. It would be interesting to understand how to apply that idea and also the recently proposed prescription of [25, 26] in the present context. Instead we simply use the Son-Starinets prescription [27–29] to compute real time correlators in the topological AdS black hole geometry, by requiring infalling boundary conditions at the horizon of the black hole.

We find that in the topological black hole phase, retarded scalar glueball correlators (homogeneous on spatial S^2 slices of dS_3) have a simple description in frequency space. They have an infinite number of poles in the lower half of the complex frequency plane. As in the case of the BTZ black hole and other well known examples, these poles represent the black hole quasinormal frequencies [27]. The Green's functions have imaginary parts and display features closely resembling thermal physics. These features are naturally associated to the Gibbons-Hawking temperature due to the cosmological horizon of de Sitter space. This suggests that the $\mathcal{N} = 4$ theory on $dS_3 \times S^1$ is in a plasma-like or deconfined state in the exponentially expanding universe.

We further investigate real time correlators involving spatial spherical harmonics of conserved R-currents to find whether they exhibit transport properties, i.e., if they relax via diffusion on the expanding spatial S^2 slices of dS_3. Applying the Son-Starinets recipe (here we have to acount for a certain subtlety involving discrete normalizable mode functions in de Sitter space) we find that the retarded propagator of the R-current does not appear to relax hydrodynamiccally. This is likely due to the "rapid" expansion of de Sitter space, the expansion rate of dS_3 being of the same order as the Gibbons-Hawking temperature. The real time correlators are represented in the form of a de Sitter mode expansion, which allows to identify a natural frequency space correlator. This latter object has isolated poles in the lower half plane and at the origin, and its imaginary part exhibits the features characteristic of a thermal state.

When the spatial circle is small (relative to the radius of curvature of dS_3), below a critical value, the topological black hole decays into the AdS bubble of nothing. In this geometry, correlation functions are not analytically calculable. However, scalar glueball propagators can be calculated in a WKB approximation. We show that in this approximation, the correlation functions have an infinite set of isolated poles on the real axis in the frequency plane. We interpret this naturally as high mass glueball-like bound states of the field theory. The transition from the topological black hole to the bubble of nothing by tunelling is interpreted as a hadronization process. A related picture of hadronization was discussed in [30].

JHEP04(2009)063

The paper is organized as follows. In section 2, we review properties of the topological AdS black hole. In section 3, we perform the detailed holographic computation of retarded propagators of the spatially homogeneous scalar glueball fields. We also calculate R-current correlation functions. Section 4 is devoted to a WKB analysis of Green's functions in the bubble of nothing phase. We summarize our results in section 5.

2 The topological AdS black hole

The so-called topological black hole of [7, 18] in AdS_5 is an orbifold of AdS space, obtained by an identification of points along the orbit of a Killing vector

$$\xi = \frac{r_\chi}{R_{\rm AdS}} \left(x_4 \partial_5 + x_5 \partial_4 \right), \tag{2.1}$$

where r_χ is an arbitrary real number and the AdS space is described as the universal covering of the hyper-surface

$$-x_0^2 + x_1^2 + x_2^2 + x_3^2 + x_4^2 - x_5^2 = -R_{\rm Ads}^2, \tag{2.2}$$

$R_{\rm AdS}$ being the AdS radius. In Kruskal-like coordinates which cover the whole spacetime, the metric has the form

$$ds^2 = \frac{4R_{\rm AdS}^2}{(1-y^2)^2}\, dy^\mu dy^\nu \eta_{\mu\nu} + \frac{(1+y^2)^2}{(1-y^2)^2}\, r_\chi^2 d\chi^2 \tag{2.3}$$

where χ is a periodic coordinate with period 2π. The four coordinates y^μ, $(\mu = 0, \dots 3)$ are non-compact with the Lorentzian norm $y^2 = y^\mu y^\nu \eta_{\mu\nu}$ such that $-1 < y^2 < 1$. Locally, the spacetime is anti-de Sitter with a periodic identification of the χ coordinate,

$$\chi \sim \chi + 2\pi. \tag{2.4}$$

The conformal boundary of the spacetime is approached as $y^2 \to 1$, and it is $dS_3 \times S^1$. The boundary conformal field theory is therefore formulated on a three dimensional de Sitter space with radius of curvature $R_{\rm AdS}$ times a spatial circle of radius r_χ.

The geometry has a horizon at $y^2 = 0$, which is the three dimensional hypercone,

$$y_0^2 = y_1^2 + y_2^2 + y_3^2, \tag{2.5}$$

and a singularity at $y^2 = -1$. The singularity appears because the region where the Killing vector has negative norm needs to be excised from the physical spacetime to eliminate closed timelike curves. The hyperboloid $y^2 = -1$ is a singularity since timelike geodesics end there and the Killing vector ∂_χ generating the orbifold identification has vanishing norm at $y^2 = -1$. The topology of the spacetime is $\mathbb{R}^{3,1} \times S^1$, in contrast to that of the AdS-Schwarzschild black hole which has the topology $\mathbb{R}^{1,1} \times S^3$. For this reason, infinity is connected in this geometry unlike in the usual Schwarzschild black hole which has two disconnected asymptotic regions.

JHEP04(2009)063

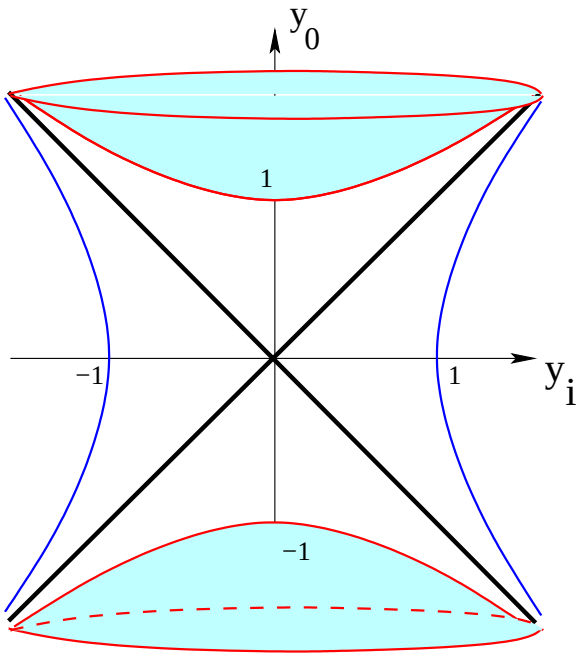

Figure 1. The global structure of the topological AdS black hole spacetime. The singularity is the hyperboloid $-y_0^2 + y_i y_i = -1$ and the horizon is at the cone $y_0^2 = y_i y_i$.

Finally, it is possible to rewrite the metric in Schwarzschild-like coordinates by introducing

$$Y^2 = \sum_{i=1}^{3} y_i y_i \,; \qquad \frac{Y}{y_0} = \coth\left(\frac{t}{R_{\rm AdS}}\right) \,; \qquad \frac{r^2}{R_{\rm AdS}^2} = 4\frac{(Y^2 - y_0^2)}{(1 + y_0^2 - Y^2)^2} \tag{2.6}$$

These coordinates only cover the region $y^2 \geq 0$ which is the exterior of the topological black hole. Locally, the metric takes the form (simply related to eq. (11) of [7] after a coordinate transformation),

$$\begin{aligned} ds^2 \,=\, & R_{\rm AdS}^2 \frac{dr^2}{(r^2 + R_{\rm AdS}^2)} + \left(\frac{r_\chi}{R_{\rm AdS}}\right)^2 (r^2 + R_{\rm AdS}^2) d\chi^2 \\ & + r^2 \left(-\frac{dt^2}{R_{\rm AdS}^2} + \cosh^2\left(\frac{t}{R_{\rm AdS}}\right) \, d\Omega_2^2 \right) . \end{aligned} \tag{2.7}$$

The Euclidean continuation of the metric yields thermal AdS space due to periodicity of the χ coordinate. Hence, the topological black hole metric (exterior to the horizon) can also be obtained following a double Wick rotation of global AdS spacetime and a periodic identification of the χ coordinate. In the Schwarzschild-like coordinates, the horizon of the topological black hole is at $r = 0$. It is clear that each slice of constant r is a $dS_3 \times S^1$ geometry. This metric, while locally describing AdS space, differs from it globally due to the identification $\chi \sim \chi + 2\pi$. Note also that the spatial S^1 remains finite sized at the horizon, with radius $R_{S^1} = r_\chi$.

JHEP04(2009)063

It is interesting to see that we can get a better understanding of the geometry in the vicinity of the singularity at $y^2 = -1$ by zooming in on the the metric (2.3) in this region. Introducing the coordinates

$$y_0 = (1-\delta)\,\cosh\varepsilon\,, \qquad Y = (1-\delta)\,\sinh\varepsilon \qquad 0 < \delta \ll 1, \tag{2.8}$$

we find

$$ds^2 \approx R^2_{\rm AdS}(-d\delta^2 + d\varepsilon^2 + \sinh^2\varepsilon\, d\Omega_2^2) + r_\chi^2\delta^2\, d\chi^2, \tag{2.9}$$

which is the metric for Milne spacetime (in the δ, χ directions).

3 Real time correlators in the topological AdS black hole

We will compute real time correlators in the Yang-Mills theory on the boundary of the topological AdS_5 black hole (TBH) following the recipe of Son and Starinets [27] in the Schwarzschild-like patch (2.7) of the black hole. Viewing the topological black hole as a Wick rotation of (Euclidean) thermal AdS space, one expects that such correlators can also be obtained by an appropriate analytic continuation of Euclidean Yang-Mills correlators on $S^3 \times S^1$ in the confined phase (the $\mathbb{Z}_N$ symmetric phase) with anti-periodic boundary conditions for fermions. Since the relevant Wick rotation turns the polar angle on S^3 into the time coordinate of de Sitter space, a complete knowledge of the angular dependence of Euclidean correlators on $S^3 \times S^1$would be necessary. However, finite temperature Yang-Mills correlators on S^3 and at strong coupling, have not been calculated explicitly, so we will not follow the route of analytic continuation. Instead we will directly calculate the real time correlators using the holographic prescription of Son and Starinets applied to the topological AdS black hole geometry.

3.1 Scalar wave equation in the topological black hole

To extract field theory correlators, we first need to look for solutions to the wave equation in the region exterior to the horizon of the topological black hole. It is instructive to write the metric for the black hole in the Schwarzschild form of [7]

$$ds^2 = R^2_{\rm AdS}\left[\frac{d\rho^2}{(\rho^2-1)} + \left(\frac{r_\chi}{R_{\rm AdS}}\right)^2 \rho^2 d\chi^2 + (\rho^2-1)\left(-d\tau^2 + \cosh^2\tau\, d\Omega_2^2\right)\right], \tag{3.1}$$

where we have introduced the dimensionless variables

$$\rho = \sqrt{(r/R_{\rm AdS})^2 + 1}, \qquad\qquad \tau = \frac{t}{R_{\rm AdS}}. \tag{3.2}$$

The conformal boundary of the space is approached as $\rho \to \infty$ while the horizon is at $\rho = 1$, where the coefficient of $d\tau^2$ vanishes. The slices with constant ρ are manifestly $dS_3 \times S^1$.

The scalar fields in this geometry have a natural expansion in terms of harmonics on the $S^2 \times S^1$ spatial slices

$$\Phi(\rho, \chi, \tau, \Omega) = \sum_{\ell,m,n} A_{\ell\, m}\, Y_{\ell\, m}(\Omega)\, e^{in\chi} \int \frac{d\nu}{2\pi}\, \Phi_n\,(\nu, \rho)\, \mathcal{T}_\ell(\nu, \tau). \tag{3.3}$$

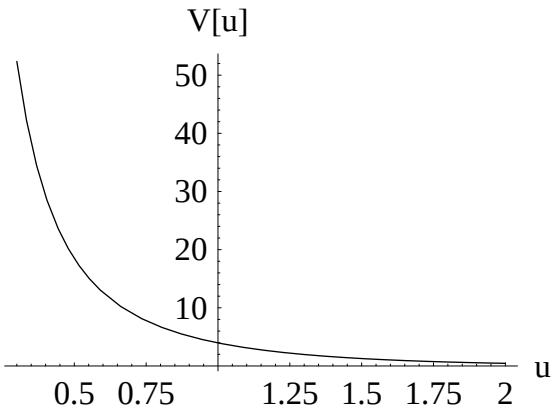

Figure 2. The Schrödinger potential for the topological AdS black hole.

The normal mode expansion above involves spherical harmonics on S^2, the discrete Fourier modes on S^1 and $\mathcal{T}_\ell(\nu,\tau)$ which solve the scalar wave equation on dS_3:

$$\frac{1}{\cosh^2\tau}\partial_\tau\left(\cosh^2\tau\,\partial_\tau\mathcal{T}_\ell(\nu,\tau)\right)+\frac{\ell(\ell+1)}{\cosh^2\tau}\mathcal{T}_\ell(\nu,\tau)=-(\nu^2+1)\mathcal{T}_\ell(\nu,\tau). \tag{3.4}$$

For every $\ell\in\mathbb{Z}$, the equation has two kinds of solutions that will be relevant for us: i) normalizable modes labelled by integers $-i\nu=1,2,\ldots\ell$; and ii) delta-function normalizable modes labelled by a continuous frequency variable $\nu\in\mathbb{R}$. We will return to this point when we discuss R-current correlators. General solutions to this equation can be expressed in terms of associated Legendre functions

$$\mathcal{T}_\ell(\nu,\tau)=\frac{1}{\cosh\tau}\left(\,A_l\;P_\ell^{i\nu}(\tanh\tau)+\;B_l\;Q_\ell^{i\nu}(\tanh\tau)\right). \tag{3.5}$$

In the usual approach to quantizing free scalar fields in de Sitter space, the integration constants A_ℓ and B_ℓ are determined by the choice of de Sitter vacuum [31–33]. However, in the present context, the constants will be specified by picking out infalling wave solutions at the horizon of the topological black hole. These are the holographic boundary conditions relevant for real time response functions in the strongly coupled field theory on $dS_3\times S^1$.

It is useful to see the scalar wave equation in this background recast as a Schrödinger equation, using Regge-Wheeler type variables

$$u=\frac{1}{2}\ln\left(\frac{\rho+1}{\rho-1}\right)\qquad\text{or}\qquad\rho=\coth u, \tag{3.6}$$

and

$$\Psi_n=\sqrt{\rho(\rho^2-1)}\,\Phi_n, \tag{3.7}$$

Φ being the scalar field in the bulk. In these coordinates, the horizon is approached as $u\to\infty$ while the conformal boundary is at $u=0$. Following the above coordinate and

JHEP04(2009)063

field redefinitions, the Schrödinger wave equation in the TBH geometry is

$$-\frac{d^2}{du^2}\,\Psi_n(\nu,u)+V_n(u)\,\Psi_n(\nu,u)=\nu^2\,\Psi_n(\nu,u), \tag{3.8}$$

$$V_n(u)=\left(\left(MR_{\rm AdS}\right)^2+\frac{15}{4}\right)\frac{1}{\sinh^2 u}+\left(\frac{1}{4}+\frac{R_{\rm AdS}^2}{r_\chi^2}\,n^2\right)\frac{1}{\cosh^2 u}\,. \tag{3.9}$$

Here, $\Psi_n=\Phi_n\sqrt{\rho(\rho^2-1)}$ and we have allowed for a generic non-zero mass M since we will eventually be interested both in the massless and massive cases. As expected for AdS black holes, the potential decays exponentially near the horizon $u\to\infty$, while blowing up near the boundary at $u\to 0$. In the near horizon region where the potential vanishes, the solutions with $\nu>0$ are travelling waves and there is a natural choice of incoming and outgoing plane wave solutions. For any n and M, the equation has analytically tractable solutions in terms of hypergeometric functions. We will use these to calculate the retarded Green's functions for the boundary gauge theory (i.e., $\mathcal{N}=4$ SYM) at strong coupling on $dS_3\times S^1$.

Although analytical solutions exist for all non-zero n and M, we will restrict attention, for simplicity, to two special cases: i) $n\neq 0$ and $MR_{\rm AdS}=0$; ii) $n=0$ and $MR_{\rm AdS}\neq 0$. In each of these two cases the radial equation is solved by two linearly independent hypergeometric functions:

$\underline{M=0;\quad n\neq 0}$

$$\begin{aligned}\Phi_n(\nu,\rho)=\;&C_1\,\rho^{-in\,R_{\rm AdS}/r_\chi}\;\times \\ &(\rho^2-1)^{-i\frac{\nu}{2}-\frac{1}{2}}\;{}_2F_1\left(-\frac{1}{2}-\frac{i}{2}\left(\nu+n\,\frac{R_{\rm AdS}}{r_\chi}\right),\;\frac{3}{2}-\frac{i}{2}\left(\nu+n\,\frac{R_{\rm AdS}}{r_\chi}\right);\;1-in\,\frac{R_{\rm AdS}}{r_\chi};\;\rho^2\right)\\ &+C_2\,\rho^{in\,R_{\rm AdS}/r_\chi}\;\times \\ &(\rho^2-1)^{-i\frac{\nu}{2}-\frac{1}{2}}\;{}_2F_1\left(-\frac{1}{2}-\frac{i}{2}\left(\nu-n\,\frac{R_{\rm AdS}}{r_\chi}\right),\;\frac{3}{2}-\frac{i}{2}\left(\nu-n\,\frac{R_{\rm AdS}}{r_\chi}\right);\;1+in\,\frac{R_{\rm AdS}}{r_\chi};\;\rho^2\right).\end{aligned} \tag{3.10}$$

Similarly, for massive fields with $n=0$, the two linearly independent solutions are

$\underline{M\neq 0;\quad n=0}$

$$\begin{aligned}\Phi_0(\nu,\rho)=\;&C_1(\rho^2-1)^{-\frac{1}{2}(4-\Delta)}\;{}_2F_1\left(\frac{1}{2}(3-\Delta)-\frac{1}{2}i\nu,\;\frac{1}{2}(3-\Delta)+\frac{1}{2}i\nu;\;3-\Delta;\;-(\rho^2-1)^{-1}\right)\\ &+C_2\,(\rho^2-1)^{-\frac{1}{2}\Delta}\;{}_2F_1\left(\frac{1}{2}(\Delta-1)-\frac{1}{2}i\nu,\;\frac{1}{2}(\Delta-1)+\frac{1}{2}i\nu;\;\Delta-1;\;-(\rho^2-1)^{-1}\right)\\ \Delta=\;&2+\sqrt{4+(MR_{\rm AdS})^2}.\end{aligned}$$

The correct linear combination, relevant for the holographic computation of correlators, is picked by applying the requirement of purely infalling waves at the horizon of the topological black hole at $\rho\approx 1$.

3.2 Scalar glueball correlator

As argued in [4, 7], the topological black hole in AdS space is automatically a solution to the Type IIB supergravity equations of motion, since it can be obtained via a double Wick

JHEP04(2009)063

rotation (and an identification) of $AdS_5 \times S^5$. The $\mathcal{N} = 4$ supersymmetric Yang-Mills theory on the $dS_3 \times S^1$ conformal boundary of the topological black hole, has two SO(6) singlet, scalar glueball fields

$$\mathcal{G}(\vec{x}, t) = \mathrm{Tr} F_{\mu\nu} F^{\mu\nu}; \qquad \tilde{\mathcal{G}}(\vec{x}, t) = \mathrm{Tr} F_{\mu\nu} \tilde{F}^{\mu\nu}. \tag{3.11}$$

These are dual to the dilaton and the RR-scalar in the Type IIB theory on the bulk spacetime and both solve the massless (corresponding to $\Delta = 4$ operators on the boundary) scalar wave equation in the topological black hole geometry. The retarded propagators for the scalar glueball fields are known on $\mathbb{R}^{3,1}$ at weak coupling both at zero and finite temperature [34]. Since the operator is chiral primary in the $\mathcal{N} = 4$ theory, at zero temperature its propagator on $\mathbb{R}^{3,1}$ receives no quantum corrections and the strong coupling results from supergravity are in exact agreement with those of the free field theory. At finite temperature, however, when supersymmetry is broken, strong and weak coupling results on $\mathbb{R}^{3,1}$ differ [27, 34]. Computations of the glueball correlator also exist in the free $\mathcal{N} = 4$ theory at finite temperature and on a spatial S^3, both in the confined and deconfined phases [34]. Their strong coupling counterparts have not been determined.

The present case, with the field theory on $dS_3 \times S^1$, is intriguing for the following reasons. First, there is the lack of supersymmetry, due to antiperiodic boundary conditions for fermions around the spatial S^1. Secondly, the boundary field theory sees a cosmological horizon on dS_3 accompanied by its thermal bath. It would be interesting to observe the emergence of the boundary Gibbons-Hawking temperature from a holographic calculation of its correlators at strong coupling. Finally, when the radius of the boundary S^1 decreases below a critical value, $r_\chi / R_{\mathrm{AdS}} \leq \frac{1}{2\sqrt{2}}$, the topological black hole decays via a bounce to the small "AdS bubble of nothing". We would like to understand how boundary field theory correlators at strong coupling on $dS_3 \times S^1$ change across this transition. The transition from the topological black hole to the Bubble of Nothing is a $\mathbb{Z}_N$ breaking transition. This is understood precisely as in the Euclidean (finite temperature) situation, due to a non-zero expectation value for the Wilson loop around the spatial S^1.

Curiously, it is apparent that in the classical supergravity approximation, the bulk scalar glueball correlators are insensitive to fermions and their boundary conditions around the spatial S^1. It would be interesting to understand whether this is related to large-N volume independence [35, 36] in the $\mathbb{Z}_N$ symmetric phase.

We are primarily interested in real time response and for the sake of simplicity, we will first study only the response functions for glueball fluctuations that are homogeneous on the spatial S^2 slices at the boundary, i.e.,

$$G_R(\tau, \tau'; n; l = 0) = -i \int \frac{d\Omega}{4\pi} \frac{d\Omega'}{4\pi} \int \frac{d\chi}{2\pi} e^{-in\chi} \Theta(\tau - \tau') \langle \left[\mathcal{G}(\Omega, \chi, \tau), \mathcal{G}(\Omega', 0, \tau') \right] \rangle. \tag{3.12}$$

We will work with the dimensionless variables $\tau = t/R_{\mathrm{AdS}}$, $\tau' = t'/R_{\mathrm{AdS}}$ and restore appropriate dimensions when necessary. As we will see when we look at R-current correlators, it is straightforward to generalize to inhomogeneous fluctuations on the spatial sphere.

For the moment we focus attention on the s-wave ($\ell = 0$) retarded correlation function of the scalar glueball operator. Also, for the s-waves, the correlator turns out to be a

function of $(\tau - \tau')$ so that it is natural to define the temporal Fourier transform of this as,

$$\tilde{G}_R(\nu\,;n) = \int_{-\infty}^{\infty} d\tau\, e^{-i\nu(\tau-\tau')}\, G_R(\tau,\tau'\,;n\,;\ell=0). \tag{3.13}$$

To calculate it at strong coupling and in the large radius regime ($r_\chi \geq \frac{R_{\rm AdS}}{2\sqrt{2}}$), we solve the dilaton wave equation which is the equation for a massless, minimally coupled scalar field in the background of the topological AdS black hole.

3.2.1 Spatially homogeneous case with $n = \ell = 0$

We begin by looking at the spatially homogeneous response functions, $l = n = 0$, on the $dS_3 \times S^1$ slices. The solutions to the radial part of the Klein-Gordon equation in the massless limit are the hypergeometric functions

$$\Phi_0^{(1)}(\nu,\rho) = \frac{\pi}{4}\,\frac{1+\nu^2}{\cosh\left(\frac{\pi\nu}{2}\right)}\;{}_2F_1\left(-\frac{1+i\nu}{2}\,,\,-\frac{1-i\nu}{2}\,;\,1\,;\,\frac{\rho^2}{\rho^2-1}\right) \tag{3.14}$$

and

$$\Phi_0^{(2)}(\nu,\rho) = (\rho^2-1)^{-2}\;{}_2F_1\left(\frac{3-i\nu}{2}\,,\,\frac{3+i\nu}{2}\,;\,3\,;\,-\frac{1}{\rho^2-1}\right). \tag{3.15}$$

For the $l = 0$ modes, the temporal dependence is also particularly simple, and has a natural interpretation in terms of positive and negative frequency states

$$\mathcal{T}_0^+(\nu,\tau) = \frac{e^{-i\nu\tau}}{\cosh\tau} \qquad \text{and} \qquad \mathcal{T}_0^-(\nu,\tau) = \frac{e^{i\nu\tau}}{\cosh\tau}. \tag{3.16}$$

Solving the Dirichlet problem and extracting correlation functions holographically requires us to first pick the correct linear combination of the two solutions which is smooth near the horizon $\rho \to 1$ and represents an incoming wave falling into the horizon. In the near horizon region, the asymptotic form of the solutions is:

$$\Phi_0^{(1)}(\nu,\rho\to 1) \to \\ i\,(2(\rho-1))^{-\frac{1-i\nu}{2}}\;e^{\frac{\pi}{2}\nu}\,\frac{\Gamma(-i\nu)\,\Gamma\left(\frac{3+i\nu}{2}\right)}{\Gamma\left(-\frac{1+i\nu}{2}\right)} + i\,(2(\rho-1))^{-\frac{1+i\,\nu}{2}}\;e^{-\frac{\pi}{2}\nu}\frac{\Gamma(i\nu)\,\Gamma\left(\frac{3-i\nu}{2}\right)}{\Gamma\left(-\frac{1-i\nu}{2}\right)} \tag{3.17}$$

and

$$\Phi_0^{(2)}(\nu,\rho\to 1) \to\; (2(\rho-1))^{-\frac{1-i\,\nu}{2}}\frac{2\,\Gamma(-i\nu)}{\Gamma\left(\frac{3-i\nu}{2}\right)^2} +\; (2(\rho-1))^{-\frac{1+i\,\nu}{2}}\frac{2\,\Gamma(i\nu)}{\Gamma\left(\frac{3+i\nu}{2}\right)^2}. \tag{3.18}$$

Note that these modes diverge as $1/\sqrt{(\rho-1)}$ near the horizon. However, employing the measure implied by the bulk metric $\sqrt{-g} \sim (\rho^2-1)^{5/2}$, these are still normalizable in the vicinity of the horizon. We can now pick a linear combination such that only incoming positive frequency waves are allowed at the horizon. This means, assuming that $\mathcal{T}_0^+$ are the positive frequency modes with $\mathrm{Re}(\nu) > 0$, the solution to the radial wave equation should

JHEP04(2009)063

behave like $(\rho-1)^{-\frac{1+i\nu}{2}}$ near the horizon. In conjunction with this we have the properly normalized boundary behaviour as $\rho\to\infty$,

$$\Phi_0^{(1)}(\nu,\rho\to\infty)\to 1+\ldots; \qquad \Phi_0^{(2)}(\nu,\rho\to\infty)\to\frac{1}{\rho^4}+\ldots. \tag{3.19}$$

The complete solution to the boundary value problem for a massless scalar with $l=n=0$, in the topological AdS black hole is then,

$$\Phi_0(\nu,\rho)=\Phi_0^{(1)}(\nu,\rho)+i\frac{\pi}{32}\,e^{\frac{\pi}{2}\nu}\,\frac{(\nu^2+1)^2}{\cosh\frac{\pi}{2}\nu}\,\Phi_0^{(2)}(\nu,\rho). \tag{3.20}$$

Following the holographic prescription [27, 28] for computing real time correlators, the Yang-Mills retarded correlation function is obtained by analyzing the boundary terms from the on-shell scalar action

$$S=\frac{N^2}{16\pi^2}\int d\tau\int d\Omega\int d\chi\; g^{\rho\rho}\sqrt{-g}\;\;\Phi(\tau,\rho)\;\partial_\rho\Phi(\tau,\rho)\;\big|_{\rho\to\infty} \tag{3.21}$$

where, for the spatial s-wave we have defined

$$\Phi(\tau,\rho)=\int_{-\infty}^{\infty}\frac{d\nu}{2\pi}\;\mathcal{T}_0^{+}(\nu,\tau)\;\Phi_0(\nu,\rho). \tag{3.22}$$

Putting together the explicit expressions for $\mathcal{T}_0^{+}(\nu,\tau)$, and the boundary behaviour of the solution (3.20) we are immediately led to the (unrenormalized) s-wave retarded correlator in frequency space, including all contact terms (finite polynomials in the frequency ν)

$$\begin{aligned}\tilde{G}_R(\nu;0)\;=\;\frac{N^2}{16\pi^2}\Bigg(&-\frac{1}{8}(1+\nu^2)^2\left[\psi\left(\frac{3-i\nu}{2}\right)+\psi\left(\frac{3+i\nu}{2}\right)-i\pi\coth\left(\pi\frac{1}{2}(\nu+i)\right)\right]\\&+\frac{1}{4}(1+\nu^2)^2\;\left(\ln\rho-\gamma_E+1\right)\big|_{\rho\to\infty}+\frac{1}{2}(1+\nu^2)\rho^2\big|_{\rho\to\infty}\Bigg).\end{aligned} \tag{3.23}$$

We remark that unlike the case of the Poincare' patch description of AdS space, the non-normalizable solution in the topological AdS black hole (akin to global AdS), contains a term proportional to $1/\rho^2$ in its near-boundary asymptotics, but it only contributes a quadratically divergent contact term in the correlation function above.

The divergent and scheme-dependent contact terms can be minimally subtracted away to yield the renormalized, retarded Green's function. Up to now we have been working with dimensionless variables, corresponding to a de Sitter boundary of unit curvature. Restoring dimensionful constants with the replacement

$$\nu\to\nu R, \tag{3.24}$$

R being the radius of curvature of the boundary dS_3 (or the inverse Hubble constant), the renormalized retarded Green's function continued into the complex frequency plane is

$$\tilde{G}_R(\nu;0)=-\frac{N^2}{64\pi^2}(R^{-2}+\nu^2)^2\;\left[\psi\left(\frac{3-i\nu R}{2}\right)-\frac{2i\nu R}{(1+\nu^2R^2)}\right]. \tag{3.25}$$

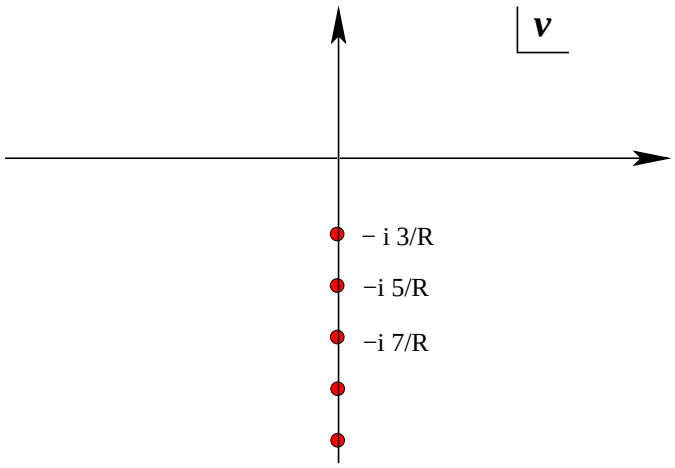

Figure 3. The analytic structure in complex frequency plane, of the massless, spatially homogeneous ($l = n = 0$), retarded Green's function in the $\mathbb{Z}_N$ symmetric phase, corresponding to the topological AdS black hole.

For $\mathrm{Im}(\nu) = 0$, its real and imaginary parts match (3.23), and the function is analytic in the upper half plane, with only isolated simple poles in the lower half plane at

$$\nu_k = -i(3+2k)\frac{1}{R} \qquad k \in \mathbb{Z} \tag{3.26}$$

As argued in [27], poles of the retarded correlator in a black hole background coincide with the quasinormal frequencies of the black hole. The quasinormal frequencies and the retarded glueball correlator found above, for the topological black hole in AdS_5, are remarkably similar to the corresponding objects in the BTZ black hole [27].

3.2.2 Non-zero momentum along S^1 and $l = 0$

It is relatively easy to allow for a non-zero discrete momentum n/r_χ along the spatial S^1. This requires the modes (3.10), to solve the boundary value problem in the topological black hole background. Following the same steps as in the s-wave correlator, (after tedious algebra) we find that the retarded Green's function (with dimensionful constants restored) is

$$\begin{aligned}\tilde{G}_R(\nu\,;n) = -\frac{N^2}{128\pi^2}\left(\left(\nu-\frac{n}{r_\chi}\right)^2+R^{-2}\right)\left(\left(\nu+\frac{n}{r_\chi}\right)^2+R^{-2}\right)\times \\ \times\left[\psi\left(\frac{3}{2}-i\frac{R}{2}\left(\nu-\frac{n}{r_\chi}\right)\right)+\psi\left(\frac{3}{2}-i\frac{R}{2}\left(\nu+\frac{n}{r_\chi}\right)\right)-\frac{2iR(\nu-\frac{n}{r_\chi})}{(\nu-\frac{n}{r_\chi})^2R^2+1}\right. \\ \left.-\frac{2iR(\nu+\frac{n}{r_\chi})}{(\nu+\frac{n}{r_\chi})^2R^2+1}\right], \qquad n\in\mathbb{Z}.\end{aligned} \tag{3.27}$$

When $n = 0$, this matches our expression for the s-wave correlator (3.25). The Green's function has nonanalyticities only in the lower half plane, with simple poles at

$$\nu_k^{\pm} = -i(3+2k)R^{-1} \pm \frac{n}{r_\chi}; \qquad k, n \in \mathbb{Z}, \tag{3.28}$$

JHEP04(2009)063

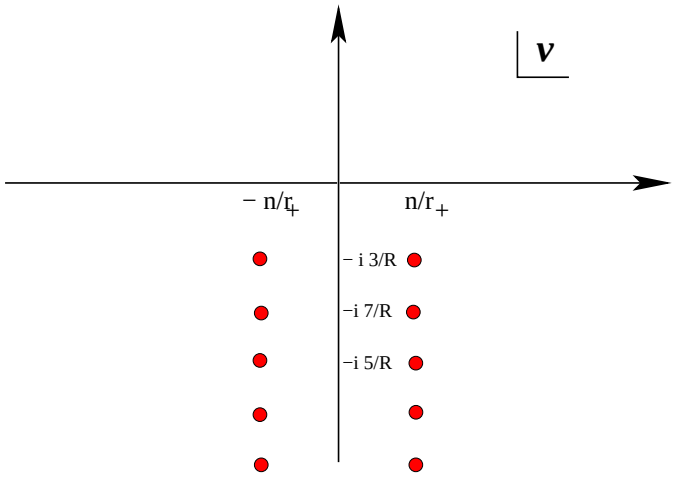

Figure 4. Simple poles in the frequency plane, of the massless retarded Green's function with non-zero momentum along the spatial circle.

giving the quasinormal frequencies of the topological black hole, with non-zero momentum along the spatial S^1. Interestingly each simple pole at $n = 0$ 'splits' into two simple poles at non-zero n. Our expressions for the correlation functions on $dS_3 \times S^1$ in the $\mathbb{Z}_N$ symmetric phase satisfy the obvious consistency check — in the high frequency/large momentum limit $\nu R, n \gg 1$, they reproduce the flat space Green's function for the scalar glueball operator

$$\tilde{G}_R(\nu\,;n)\Big|_{\nu R,\, n\gg 1} \longrightarrow -\frac{N^2}{128\pi^2}\left(\nu^2-\frac{n^2}{r_\chi^2}\right)^2 \ln\left(\nu^2-\frac{n^2}{r_\chi^2}\right). \tag{3.29}$$

3.3 Thermal effects and the Gibbons-Hawking temperature

De Sitter space has a cosmological horizon and an associated Gibbons-Hawking temperature [23]. We therefore expect our boundary ($dS_3 \times S^1$) field theory correlators to exhibit thermal properties. For real frequencies ν, the digamma functions have an imaginary part so that

$$\begin{aligned}\mathrm{Im}\,\tilde{G}_R(\nu\,;n)\Big|_{\mathrm{Im}(\nu)=0} = \frac{N^2}{256\pi}&\left(\left(\nu-\frac{n}{r_\chi}\right)^2+R^{-2}\right)\left(\left(\nu+\frac{n}{r_\chi}\right)^2+R^{-2}\right)\times \\ &\left[\coth\left(\frac{\pi R}{2}\left(\nu+\frac{n}{r_\chi}-iR^{-1}\right)\right)+\coth\left(\frac{\pi R}{2}\left(\nu+\frac{n}{r_\chi}-iR^{-1}\right)\right)\right]\end{aligned} \tag{3.30}$$

Here we have used $\tanh(x) = \coth(x + i\frac{\pi}{2})$, to cast the result in a form that will make the connection to thermal physics explicit.

In *flat space* and in free field theory at finite temperature $T \neq 0$, the scalar glueball propagator , with zero spatial momentum and frequency ω is proportional to the digamma function [34]

$$\tilde{G}_R(\omega)\big|_{\text{Flat space}} = -\frac{N^2}{2\pi^2}\,\omega^4\psi\left(\frac{-i\omega}{4\pi T}\right) + \text{analytic}. \tag{3.31}$$

The imaginary part of the flat space glueball correlator is the spectral function

$$\mathrm{Im}\,\tilde{G}_R(\omega)\big|_{\text{Flat space}} = -\frac{N^2}{2\pi^2}\omega^4\pi\coth\left(\frac{\omega}{4T}\right). \tag{3.32}$$

In weakly coupled, or free field theories at finite temperature (on flat space), the one-loop spectral function reflects the physical effect of 'Bose enhancement', following from stimulated emission of bosons into the heat bath. In perturbative field theory on flat space, this manifests itself as an enhancement of the decay rate of an unstable boson in a heat bath, at rest with energy ω, by a factor (relative to the vacuum decay rate)

$$\coth\left(\frac{\omega}{4T}\right) = 1 + 2n_B\left(\frac{\omega}{2}\right) = 1 + \frac{2}{e^{\omega/2T} - 1}. \tag{3.33}$$

While there may not be an obvious way define a spectral representation in de Sitter space, the similarity between our strongly coupled de Sitter space result (3.30) and (3.32) is obvious. In particular, it allows the identification of a temperature in de Sitter space

$$T_H = \frac{R^{-1}}{2\pi} \tag{3.34}$$

which is precisely the value of the Gibbons-Hawking temperature. Note that despite the similarity between the expressions for dS_3 and thermal correlators in flat space, there is a crucial difference — the frequency or 'energy' appearing in the Bose-Einstein-like distribution function in de Sitter space, is not the real frequency ν (3.30), but in fact $\nu - iR^{-1}$. This difference can be traced back to the definition of our positive and negative frequency modes (3.16). For real ν, the positive frequency modes are red-shifted away in the far future. To get propagating modes in the future, we would need to choose $\nu = \omega + iR^{-1}$ with $\omega \in \mathbb{R}$.

It is interesting to note that our results for the retarded glueball propagator in the strongly coupled field theory (in the $\mathbb{Z}_N$ symmetric phase) on de Sitter space closely match one-loop weakly coupled field theory calculations [37]. It would be a straightforward calculation to check whether there is exact agreement between weak and strong coupling results on $dS_3 \times S^1$. We leave this excercise for the future. For now, we only make the following observation, which suggests that the scalar glueball correlator in the $\mathbb{Z}_N$ symmetric phase should not be renormalized.

It has been argued in [35, 36] that correlation functions of large N gauge theories in the $\mathbb{Z}_N$ symmetric phase, with some or all spacetime directions compactified, should be independent of the volume of the compact directions. In the present situation this would imply that on $dS_3 \times S^1$ with antiperiodic boundary conditions for the fermions, large N correlators in the $\mathbb{Z}_N$ symmetric phase ($r_\chi > R_{\rm AdS}/2\sqrt{2}$) should be independent of the radius of the S^1. In particular then, for perturbations which are homogeneous along the circle, the correlation functions should be independent of r_χ and should match up with the result on $dS_3 \times \mathbb{R}$. The latter is obtained by a (double) Wick rotation of $S^3 \times \mathbb{R}$. Since $\mathrm{Tr}F^2$ is a chiral primary in the $\mathcal{N} = 4$ theory and its correlator on $S^3 \times \mathbb{R}$ is not renormalized by interactions, one would expect this to be true also on $dS_3 \times \mathbb{R}$.

3.4 The massive case

The holographic calculation of correlation functions in the topological AdS black hole can be easily extended to massive scalars. In the context of the Type IIB theory, such massive

JHEP04(2009)063

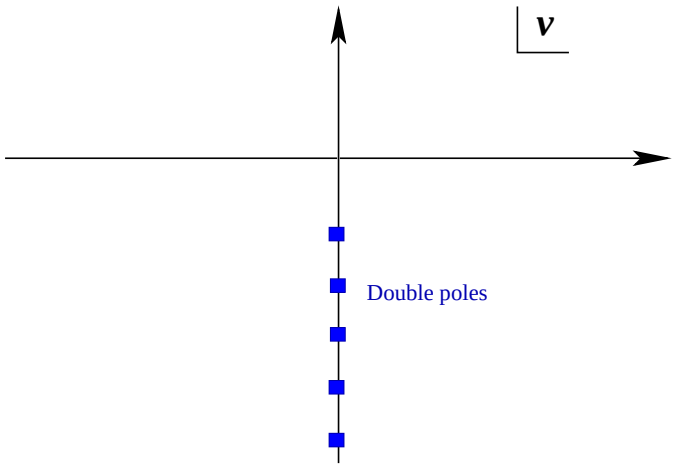

Figure 5. Double poles in the lower half plane for the massive (retarded) propagator at zero spatial momentum.

states are stringy excitations with masses $M^2 \sim \alpha'^{-1} \gg R_{\rm AdS}^{-2}$. A scalar field of mass M in the bulk is dual to a scalar operator $\mathcal{O}_\Delta$ in the field theory with conformal dimension $\Delta = 2+\sqrt{4+(MR_{\rm AdS})^2}$. We will study below the free massive scalar in the bulk geometry to extract information on the analytic structure of correlators of high dimension operators in the field theory.

There are two primary motivations for looking at high dimension operators in the field theory: i) The works of [38, 39] have demonstrated that propagators of heavy fields, in the geodesic approximation, may be used to probe the bulk geometry behind horizons and perhaps extract information on singularities behind such horizons. ii) One of our main goals is to look for signatures of the transition between a $\mathbb{Z}_N$ symmetric phase and a $\mathbb{Z}_N$ broken phase. In the bulk theory, the latter phase is the small bubble-of-nothing geometry. Correlators in this latter geometry can only be computed using an eikonal (WKB) approximation involving high frequencies and/or large masses.

Extending the holographic analysis done above for massless fields, to massive scalars in the topological black hole geometry, we find that the frequency space correlator is

$$\tilde{G}_R(\nu) = \mathcal{C}_\Delta \, \frac{\Gamma\left(\frac{1}{2}\left(\Delta - 1 - i\nu R\right)\right)^2 \Gamma\left(3-\Delta\right)}{\Gamma\left(\frac{1}{2}\left(3 - \Delta - i\nu R\right)\right)^2 \Gamma(\Delta - 1)}, \tag{3.35}$$

where the normalization constant $\mathcal{C}_\Delta = 2(\Delta-2)\epsilon^{2(\Delta-4)}$, with $\epsilon \to 0$ as the boundary is approached.

In the massless limit $MR \to 0$, this reproduces the expression (3.25) found previously, after subtracting an additional divergent contact term. The massive correlator has an analytic structure that is qualitatively distinct from the massless case. In particular the retarded correlator has an infinite set of *double poles* and *simple poles* at

$$\nu_k = -i(\Delta - 1 + 2k)\frac{1}{R}\,; \qquad k \in \mathbb{Z}. \tag{3.36}$$

JHEP04(2009)063

The significance of the appearance of double poles in the massive retarded propagator is not entirely clear. Such double poles have also appeared in 2d CFT correlators with non-integer conformal dimensions from the BTZ black hole [27], at zero spatial momentum. At finite spatial momentum (e.g. $n \neq 0$) we expect the double poles to split into simple poles.

For real frequencies, the massive correlator also has an imaginary part

$$\text{Im}\, \tilde{G}_R(\nu) = -\frac{\pi^2}{2}\mathcal{C}_\Delta \frac{\Gamma(3-\Delta)}{\Gamma(\Delta-1)} \frac{\sin(\pi\,\Delta)\ \sinh(\pi\,\nu R)}{|\Gamma\left(\frac{1}{2}(3-\Delta-i\nu R)\right)\cos\left(\frac{\pi}{2}(\Delta-i\nu R)\right)|^4}. \tag{3.37}$$

The (de Sitter) thermal origin of this result is not as explicit as for the massless scalar. However, after identifying the de Sitter Hawking temperature to be $T_H = R^{-1}/2\pi$, it is worth comparing the above expression with the imaginary part of the propagator in two dimensions for large non-integer conformal dimension deduced from the non-extremal BTZ black hole [27]. The similarities between the two results, particularly the numerator of (3.37), are striking.

The large mass, high frequency limit of this result is easily obtained, using Stirling's approximation

$$\Gamma(z)\big|_{z\gg 1} \simeq \sqrt{2\pi}\frac{1}{\sqrt{z}}\, e^{-z}\, z^z. \tag{3.38}$$

When the masses are taken to be large so that $MR \gg 1$, then $\Delta \approx MR$. In this high frequency, large mass limit it is useful to define a rescaled frequency variable

$$\tilde{\nu} \equiv \frac{\nu}{M}; \qquad \nu R,\ MR \gg 1, \tag{3.39}$$

so that

$$G_R(\tilde{\nu}) \sim \mathcal{C}_\Delta \left(\frac{1-i\tilde{\nu}}{2}\right)^{MR(1-i\tilde{\nu})} \left(\frac{-1-i\tilde{\nu}}{2}\right)^{MR(1+i\tilde{\nu})}. \tag{3.40}$$

Here we have ignored an overall (real) phase due to frequency independent coefficients in the large mass limit. At first sight, a potentially problematic feature of this approximation is that there is a branch point singularity at $\tilde{\nu} = +i$ which would imply a non-analyticity in the upper half plane, inconsistent with the definition of a retarded propagator. Note that this feature is purely a result of the high frequency approximation and the exact result (3.35) has no singularities in the upper half of the complex frequency plane. Indeed, closer inspection reveals that the putative branch cut originating at $\tilde{\nu} = +i$ has a vanishing discontinuity in the limit of large MR. The spurious branch cut originates from the equally spaced zeroes of $G_R(\nu)$ appearing to coalesce in the high frequency limit. The branch cut discontinuity at $\tilde{\nu} = -i$ is, however a genuine non-analyticity and originates from the infinite set of poles merging into a continuum in the high frequency approximation. The easiest way to understand the singularities and discontinuities of the function above, is to examine the function $z^{2MRz}\ (z-1)^{-2MR(z-1)}$ and then make the replacement $z \to (1-i\tilde{\nu})/2$.

JHEP04(2009)063

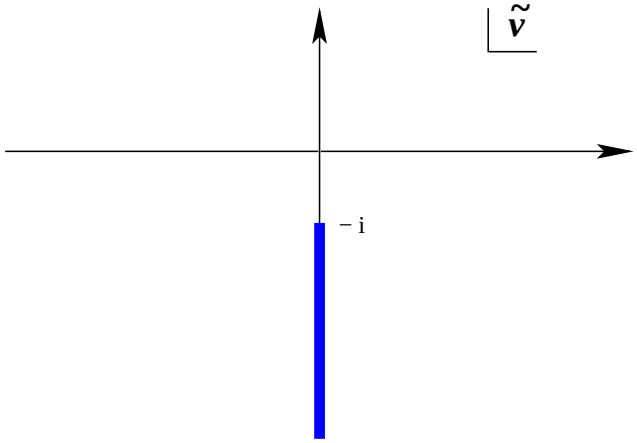

Figure 6. For large mass and frequency, the propagator in the topological black hole phase, has a branch cut as indicated in the rescaled frequency plane, $\tilde{\nu} = \nu/M$. This results from the apparent merging of the infinite set of isolated poles of the exact Green's function.

Along the branch cut $\mathcal{B} \equiv \{\tilde{\nu} \in [-i, -i\infty)\}$, we find that the retarded propagator has a discontinuity

$$\begin{aligned} \text{Disc}|_{\mathcal{B}}\, \tilde{G}_R(M\tilde{\nu}) =& 2i\, \mathcal{C}_\Delta\ \sin(2\pi MR) \left(\frac{|\tilde{\nu}|+1}{2}\right)^{MR(|\tilde{\nu}|+1)} \left(\frac{|\tilde{\nu}|-1}{2}\right)^{-MR(|\tilde{\nu}|-1)} \\ & \tilde{\nu} = -\, i|\tilde{\nu}|\,, \\ & |\tilde{\nu}| \geq 1. \end{aligned}$$

It is clear that the discontinuity is large in the large mass limit.

Now let us look closely at the putative branch cut along the imaginary axis $\mathcal{B}' \equiv \{\tilde{\nu} \in [-i, i]\}$. Computing the discontinuity across this, we have

$$\begin{aligned} \text{Disc}|_{\mathcal{B}'}\, \tilde{G}_R(M\tilde{\nu}) =& 2i\, \mathcal{C}_\Delta \sin\left(MR\pi(1-x)\right) \left(\frac{1+x}{2}\right)^{MR(1+x)} \left(\frac{1-x}{2}\right)^{MR(1-x)}; \\ & \tilde{\nu} = ix, \\ & -1 \leq x \leq 1. \end{aligned}$$

This vanishes when $MR \to \infty$, for two reasons. The rapid sinusoidal oscillations will give vanishing contribution to any contour integral along $\mathcal{B}'$. Furthermore the amplitude of the oscillations vanishes exponentially as evident from the expression above.

In the leading high frequency approximation , for real frequencies, the imaginary and real parts of the Green's function are given by

$$\begin{aligned} \tilde{G}_R(\nu) \approx \mathcal{C}_\Delta\ & \left(\frac{\nu^2+M^2}{4M^2}\right)^{MR} e^{-\frac{1}{\pi}\frac{\nu}{T_H}\tan^{-1}\frac{\nu}{M}}\ e^{-\frac{|\nu|}{2T_H}} \left(\cos\left(\frac{M}{2T_H}\right) - i\,\text{sgn}(\nu)\sin\left(\frac{M}{2T_H}\right)\right), \\ & T_H = \frac{R^{-1}}{2\pi}\,, \quad \nu \in \mathbb{R}. \end{aligned} \tag{3.41}$$

The high frequency, large mass limit thus appears to retain features of the thermal effects of de Sitter space. This result can be deduced from (3.40) after choosing an appropriate branch of the function and also directly follows from (3.37). We will see subsequently that these high frequency expressions can also be derived by solving the wave equations using a WKB approximation, providing a consistency check.

3.5 R-current correlation functions

Real time response to perturbations of a conserved charge density can reveal interesting late time physics, such as hydrodynamic or diffusive relaxation. It is now well understood and established [28, 29] via holographic calculations in AdS black hole backgrounds, that correlators of conserved global currents exhibit hydrodynamic and diffusion poles. R-charge diffusion in the strongly coupled, high temperature $\mathcal{N} = 4$ plasma was first discovered in [28]. The universal features of strongly coupled plasmas follow from the properties of the stretched horizon of AdS black holes [29]. It is therefore natural to ask whether the horizon in the topological AdS black hole geometry implies hydrodynamic behaviour of correlation functions in the dual field theory. The answer to this question will depend on the relevant time scales involved since the boundary field theory is formulated on an expanding background, namely $dS_3 \times S^1$.

The strong coupling correlators for SO(6) R-currents of $\mathcal{N} = 4$ SUSY Yang-Mills theory on $dS_3 \times S^1$ will be obtained holographically from the on-shell action for the $\mathrm{SO}(6)_R$ gauge fields in the topological AdS_5 black hole background, by following the prescription of [28]. The Maxwell action for the gauge field is

$$S = -\frac{1}{4g_{\mathrm{SG}}^2}\int d^5x\sqrt{-g}g^{\mu\alpha}g^{\nu\beta}F_{\mu\nu}F_{\alpha\beta}, \tag{3.42}$$

varying which gives the following equations of motion

$$\frac{1}{\sqrt{-g}}\partial_\nu\left(\sqrt{-g}g^{\mu\alpha}g^{\nu\beta}F_{\alpha\beta}\right) = 0. \tag{3.43}$$

Here, we have $g_{\mathrm{SG}}^2 = 16\pi^2 R_{\mathrm{AdS}}/N^2$. We find it convenient to use the following form for the metric in the region exterior to the horizon,

$$ds^2 = \frac{R_{\mathrm{AdS}}^2}{4z^2\,(1-z)}dz^2 + \frac{R_{\mathrm{AdS}}^2(1-z)}{z}\left[-d\tau^2 + \cosh^2\tau\; d\Omega_2^2\right] + \frac{r_\chi^2}{z}\,d\chi^2. \tag{3.44}$$

Substituting the solution to the equation of motion that corresponds to the boundary value $A_\alpha(z)\big|_{z=0} = A_\alpha^0$ back into the gauge field action, we will get a generating functional for the R-charge correlators of the field theory.

Since the field theory lives on the $dS_3 \times S^1$ boundary with spatial $S^2 \times S^1$ spatial slices, it is natural to consider the late time behaviour of long-wavelength fluctuations in the following two cases:

1. The R-charge perturbation is inhomogeneous on the S^1, but homogeneous on the spatial section of dS_3,

JHEP04(2009)063

2. The fluctuation is homogeneous on the circle, but inhomogeneous on the S^2.

Of particular interest is the presence or the lack of late time hydrodynamic relaxation of this system.

3.5.1 Inhomogeneous perturbation on the S^1

In the first case, we will assume, for simplicity that the R-charge perturbation carries no momentum around the S^2. Furthermore, we use gauge freedom to set the radial component of the gauge potential $A_z = 0$. Hence, from the symmetries of the configuration, there are two remaining bulk gauge fields that are non zero:

$$A_\tau = A_\tau(z,\tau,\chi), \qquad A_\chi = A_\chi(z,\tau,\chi). \tag{3.45}$$

Since the χ-direction is a spatial circle, the two components of the vector potential, A_τ and A_χ, can be conveniently expanded in Fourier modes on the circle. The time dependence can also be re-expressed in terms of a mode expansion. There is a subtlety involved in this however. For A_χ, which is a scalar in dS_3, the mode decomposition is straightforward

$$A_\chi(z,\tau,\chi) = \sum_n \frac{e^{in\chi}}{2\pi} \int_{-\infty}^{\infty} \frac{d\nu}{2\pi}\, \mathcal{T}_\chi(\nu,\tau)\ \mathcal{G}_n(\nu,z), \tag{3.46}$$

where $n \in \mathbb{Z}$. On the other hand A_τ, which is a gauge field in dS_3, has its complete time dependence captured by normal modes of two kinds — normalizable and delta-function normalizable. In fact, below we show that there is a single normalizable mode and a continuum of delta-function normalizable states obtained as solutions to a Schrödinger problem. Anticipating this we write

$$A_\tau(z,\tau,\chi) = \sum_n \frac{e^{in\chi}}{2\pi} \left(\int_{-\infty}^{\infty} \frac{d\nu}{2\pi}\, \mathcal{T}_\tau(\nu,\tau)\ \mathcal{F}_n(\nu,z) + \mathcal{T}_\tau^{\rm N}(\tau)\, \mathcal{F}_n^{\rm N}(z) \right), \tag{3.47}$$

where $\mathcal{T}_\tau(\nu,\tau)$ and $\mathcal{T}_\tau^{\rm N}(\tau)$ will be the delta-normalizable and normalizable modes respectively. The mode functions $\mathcal{T}_{\chi,\tau}$ are solutions to

$$\frac{d}{d\tau}\left(\cosh^{-2}\tau\, \frac{d}{d\tau}\left(\cosh^2\tau\, \mathcal{T}_\tau(\nu,\tau) \right) \right) = -(\nu^2+1)\ \mathcal{T}_\tau(\nu,\tau), \tag{3.48a}$$

$$\cosh^{-2}\tau \frac{d}{d\tau}\left(\cosh^2\tau\, \mathcal{T}_\tau \right) = -i(\nu+i)\mathcal{T}_\chi.$$

The first of these can be put in the form of a Schrödinger equation, by defining $\mathcal{T}_\tau = \tilde{\mathcal{T}}/\cosh\tau$,

$$-\frac{d^2}{d\tau^2}\tilde{\mathcal{T}} - \frac{2}{\cosh^2\tau}\tilde{\mathcal{T}} = \nu^2\, \tilde{\mathcal{T}}. \tag{3.49}$$

It is solved by the associated Legendre function $P_1^{-i\nu}(\tanh\tau)$. For $\nu^2 \geq 0$, there is a continuous infinity of delta-function normalizable states, which yield

$$\mathcal{T}_\tau(\nu,\tau) = \frac{e^{-i\nu\tau}}{\cosh\tau}\left(\frac{\nu - i\tanh\tau}{\nu - i} \right), \qquad \mathcal{T}_\chi(\nu,\tau) = \frac{e^{-i\nu\tau}}{\cosh\tau}, \qquad \nu^2 \geq 0. \tag{3.50}$$

The Schrödinger potential above also has bound states for $\nu^2 < 0$. In fact there is precisely one normalizable bound state with $\nu^2 = -1$, corresponding to the solution

$$\mathcal{T}_\tau^{\rm N}(\tau) = \frac{1}{\sqrt{2}}\,\frac{1}{\cosh^2\tau}. \tag{3.51}$$

This solution can be directly obtained by evaluating $P_1^{-i\nu}(\tanh\tau)$ at $\nu^2 = -1$ (and appropriately normalized) or can be systematically inferred from the Maxwell equations. The continuum modes for A_χ and A_τ are orthonormal with respect to the inner product

$$\langle \mathcal{T}_a, \mathcal{T}_a\rangle \equiv \int_{-\infty}^{\infty} d\tau \cosh^2\tau\; \mathcal{T}_a(\nu,\tau)\mathcal{T}_a(\nu',\tau) = 2\pi\,\delta(\nu+\nu'), \tag{3.52}$$

for $a \in \{\chi,\tau\}$, while the bound state is normalized so that

$$\int_{-\infty}^{\infty} d\tau\; \cosh^2\tau\; \left(\mathcal{T}_\tau^{\rm N}\right)^2 = 1. \tag{3.53}$$

In the far future the continuum modes are both given by $\mathcal{T}_a \sim e^{-i\nu\tau}e^{-2\tau}$. Upon analytically continuing to the complex ν plane, for $\nu = i+\omega$, with $\omega \in \mathbb{R}$, they are propagating (purely oscillatory) excitations with frequency ω in the far future. On the other hand the (normalizable) bound state decays exponentially in the far past and future and being real does not contribute to the flux at the horizon of the topological black hole.

Using these modes to eliminate the τ-dependence we find three equations that depend only on $\mathcal{F}_n(\nu,z)$ and $\mathcal{G}_n(\nu,z)$

$$-\frac{1}{R_{\rm AdS}^2}\,(\nu+i)\,\mathcal{F}_n' + \frac{n(1-z)}{r_\chi^2}\,\mathcal{G}_n' = 0, \tag{3.54a}$$

$$\frac{1}{R_{\rm AdS}^2}\frac{d}{dz}\left((1-z)\mathcal{F}_n'\right) + \frac{n}{r_\chi^2}\,(\nu-i)\,\mathcal{G}_n - \frac{n^2}{r_\chi^2}\,\mathcal{F}_n = 0, \tag{3.54b}$$

$$4z\frac{d}{dz}\left((1-z)^2\mathcal{G}_n'\right) - n(\nu+i)\mathcal{F}_n + (\nu^2+1)\mathcal{G}_n = 0. \tag{3.54c}$$

Here, prime denotes a derivative with respect to z. The radial or z-dependence of the bound state solution, $\mathcal{F}^{\rm N}(z)$ is found by analytically continuing the profile for generic ν to $\nu = \pm i$. Note that there are three equations for two unknowns; so, to ensure a non-trivial solution any two equations must imply the third and it is straightforward to check that this is indeed the case. We can then use these equations of motion to derive two independent ones, each containing only one of the unknown functions:

$$4z(1-z)\mathcal{F}_n''' - 4(3z-1)\mathcal{F}_n'' - 4\mathcal{F}_n' = \left[\bar{n}^2 - \frac{\nu^2+1}{1-z}\right]\mathcal{F}_n', \tag{3.55a}$$

$$4z(1-z)\mathcal{G}_n''' - 4(5z-1)\mathcal{G}_n'' - \frac{8(1-2z)}{1-z}\mathcal{G}_n' = \left[\bar{n}^2 - \frac{(\nu^2+1)}{1-z}\right]\mathcal{G}_n', \tag{3.55b}$$

where we have defined $\bar{n} \equiv \frac{nR_{\rm AdS}}{r_\chi}$. These equations are immediately solved in terms of hypergeometric functions. Singling out the solutions that satisfy the purely infalling wave boundary condition at the horizon, we find the induced boundary action for the Maxwell

JHEP04(2009)063

fields (see appendix A for details). The R-current correlators can be read off from the finite and non-analytic pieces of this boundary action (A.8), (A.12). We will denote the Fourier harmonics of the R-current along the spatial circle as

$$j_n^\mu(\tau) = \int_0^{2\pi} d\chi\, e^{-in\chi}\, j^\mu(\chi,\tau), \tag{3.56}$$

where we have already restricted attention to the s-wave sector on the spatial two-sphere. For perturbations with non-vanishing momentum along the spatial circle, we define the retarded, real time, Green's functions as

$$G^{\mu\nu}(\tau,\tau';n) = \langle [\, j_n^\mu(\tau),\, j_{-n}^\nu(\tau')]\rangle\, \Theta(\tau-\tau')\,, \qquad \mu,\nu\in\{\chi,\tau\}. \tag{3.57}$$

The conserved global currents are in one-to-one correspondence with the boundary values of the 5-d gauge fields. Functionally differentiating the induced boundary action (A.12) with respect to the boundary values of the gauge fields, we find

$$\begin{aligned}
G^{\tau\tau}(\tau,\tau';n) =& \cosh^2\tau\cosh^2\tau'\times \qquad\qquad (3.58a)\\
& n^2\left[\int_{-\infty}^{\infty}\frac{d\nu}{2\pi}\,\mathcal{T}_\tau(\nu,\tau)\mathcal{T}_\tau(-\nu,\tau')\;\Xi(\nu,n)+\mathcal{T}_\tau^{\rm N}(\tau)\mathcal{T}_\tau^{\rm N}(\tau')\;\Xi(i,n)\right],\\
G^{\chi\chi}(\tau,\tau';n) =& \cosh^2\tau\cosh^2\tau'\int_{-\infty}^{\infty}\frac{d\nu}{2\pi}\,\mathcal{T}_\chi(\nu,\tau)\mathcal{T}_\chi(-\nu,\tau')\,(\nu^2+1)\;\Xi(\nu,\,n), \qquad (3.58b)\\
G^{\tau\chi}(\tau,\tau';n) =& G^{\chi\tau\,*}(\tau,\tau';n) \qquad\qquad (3.58c)\\
=& \cosh^2\tau\cosh^2\tau'\,n\int_{-\infty}^{\infty}\frac{d\nu}{2\pi}\,\mathcal{T}_\tau(\nu,\tau)\mathcal{T}_\chi(-\nu,\tau')\,(\nu-i)\,\Xi(\nu,n),\\
\Xi(\nu,\,n) =& \frac{N^2R_{\rm AdS}}{32\pi^2 r_\chi}\left(\psi\left(\frac12+\frac{i}{2}(\bar n-\nu)\right)+\psi\left(\frac12-\frac{i}{2}(\bar n+\nu)\right)\right). \qquad (3.58d)
\end{aligned}$$

It is easily established that the above expressions are indeed retarded Green's functions and are non-vanishing only when $\tau>\tau'$. Two essential features ensure that this is the case: The function $\Xi(\nu,n)$ appearing universally in the ν-integrals has only simple poles in the lower half complex plane at

$$\nu = -i(2k+1)\pm\bar n\,, \qquad k\in\mathbb{Z}. \tag{3.59}$$

There is a second source of non-analyticities in the ν-plane. This lies in the ν-dependent normalization of the mode functions $\mathcal{T}_\tau(\nu,\tau)$ (3.50). The potentially worrisome aspect of this is the appearance of a pole in the *upper* half plane at $\nu=+i$, which gives a non-vanishing contribution for $\tau<\tau'$. However, the potential problem is eliminated by the term dependent on the discrete, normalizable mode $\mathcal{T}_\tau^N$ in (3.58a) which exactly cancels against the contributions from the poles at $\nu=+i$, ensuring that our Green's function is causal. The remaining Green's functions are manifestly free of singularities in the upper half plane.

We thus see that the Son-Starinets recipe for determining real time response functions works in the case of the topological black hole, provided we carefully account for the contributions from both the continuum and discrete mode functions in dS_3.

JHEP04(2009)063

It is also clear in the above expressions, that there are no diffusion poles. Instead, from the properties of the digamma function which we have encountered before, the frequency space Green's function which is effectively $\Xi(\nu, n)$, has only simple poles in the complex ν-plane, the lowest of these being at

$$\nu = -i \pm \bar{n}. \tag{3.60}$$

Excitations with complex $\nu = \omega - i$, and $\omega \in \mathbb{R}$ will propagate at late times, the perturbations simply evolving as left- and right-moving excitations on the S^1 without dissipating.

The absence of any diffusion or transport like behaviour may be intuitively explained by noticing the similarity of the topological AdS black hole to the BTZ black hole Setting up an excitation with momentum only on the S^1 is equivalent to saying the variation of the fields along the S^2 is zero. Therefore, aside from the time dependent factors associated to the de Sitter expansion, the metric that is "seen" by the bulk fields is not the full five dimensional metric, but its effective $2+1$ dimensional portion,

$$ds^2 = -R^2_{\rm AdS}(\rho^2 - 1)d\tau^2 + \frac{R^2_{\rm AdS}}{\rho^2 - 1}d\rho^2 + \rho^2 r_\chi^2 d\chi^2 \tag{3.61}$$

Comparing this with the metric for a $2+1$ dimensional BTZ black hole with zero angular momentum

$$ds^2 = -\left(\frac{r^2}{R^2} - M\right)dt^2 + \left(\frac{r^2}{R^2} - M\right)^{-1} dr^2 + r^2 d\phi^2, \tag{3.62}$$

we note the obvious similarity. Therefore we expect the behaviour of fields in the topological black hole background with an inhomogeneous excitation around the S^1, to be similar to the behaviour of the fields in a BTZ black hole background. In other words, they should behave as in a (1+1)-dimensional CFT [27], just as we see from our results above.

3.5.2 Inhomogeneous perturbation on the S^2

We will now examine the real time response to fluctuations carrying momentum along the spatial sections of three dimensional de Sitter space. Each spatial section of dS_3 is a two-sphere which undergoes exponential expansion at late times. For this case, we will focus on a situation where an inhomogeneous R-charge perturbation is set up on the two-sphere with only a dependence on the polar angle θ and time τ. For this configuration, the dual bulk gauge fields are

$$A_\tau = A_\tau(z, \tau, \theta)\,; \qquad A_\theta = A_\theta(z, \tau, \theta)\,; \qquad A_z = A_\chi = 0, \tag{3.63}$$

where A_z is set to zero by the gauge freedom, and A_χ vanishes due to χ-independence of the configuration. By spherical symmetry, the scalar potential A_τ and the vector potential A_θ, each can be expanded in terms of scalar and vector spherical harmonics, respectively:

$$A_\tau = \sum_{\ell=0}^{\infty} \mathcal{F}_\ell(z, \tau)\, Y^0_\ell(\theta), \qquad A_\theta = \sum_{\ell=1}^{\infty} \mathcal{G}_\ell(z, \tau)\, \partial_\theta Y^0_\ell(\theta). \tag{3.64}$$

Substituting these into the bulk Maxwell equations, we find

$$4z(1-z)\partial_z\left((1-z)\partial_z\mathcal{G}_\ell\right)-\partial_\tau^2\mathcal{G}_\ell+\partial_\tau\mathcal{F}_\ell=0 \tag{3.65a}$$

$$4z(1-z)\partial_z\left((1-z)\partial_z\mathcal{F}_\ell\right)-\frac{\ell(\ell+1)}{\cosh^2\tau}\left(\mathcal{F}_\ell-\partial_\tau\mathcal{G}_\ell\right)=0, \tag{3.65b}$$

$$\partial_\tau\left(\cosh^2\tau\,\partial_z\mathcal{F}_\ell\right)+\ell(\ell+1)\partial_z\mathcal{G}_\ell=0. \tag{3.65c}$$

From equations (3.65b) and (3.65c) we obtain a differential equation for $\mathcal{F}'_\ell\equiv\partial_z\mathcal{F}_\ell$

$$4\partial_z\left(z(1-z)\partial_z\left((1-z)\mathcal{F}'_\ell\right)\right)-\frac{\ell(\ell+1)}{\cosh^2\tau}\mathcal{F}'_\ell-\frac{1}{\cosh^2\tau}\partial_\tau^2\left(\cosh^2\tau\,\mathcal{F}'_\ell\right)=0. \tag{3.66}$$

Now we will separate out the explicit temporal dependence, keeping in mind, as before, the possibility of contributions from both discrete and continuous modes

$$\mathcal{F}'_\ell(z,\tau)=\int_{-\infty}^{\infty}d\nu\;\mathcal{T}_\ell(\nu,\tau)\;F_\ell(\nu,z)+\sum_m\mathcal{T}^{\rm N}_{\ell m}(\tau)\,F^{\rm N}_{\ell m}(z). \tag{3.67}$$

The mode functions $\mathcal{T}_\ell$ satisfy

$$\left[-\partial_\tau^2-\frac{\ell(\ell+1)}{\cosh^2\tau}\right]\left(\cosh^2\tau\,\mathcal{T}_\ell\right)=\nu^2\;\left(\cosh^2\tau\,\mathcal{T}_\ell\right), \tag{3.68}$$

which is a Schrödinger equation whose potential clearly will have both bound states and scattering or continuum states. The full set of solutions form an orthonormal, complete set. Indeed, the delta-normalized eigenstates are the Legendre functions

$$\mathcal{T}_\ell(\nu,\tau)=\Gamma(1+i\nu)\,\frac{P_\ell^{-i\nu}(\tanh\tau)}{\cosh^2\tau}. \tag{3.69}$$

Those with $\nu^2>0$ are scattering states with continuous values of $\nu\in\mathbb{R}$, while the discrete, "bound states" have $-i\nu=1,2,\dots\ell$,

$$\mathcal{T}^{\rm N}_{\ell m}=\sqrt{\frac{m(\ell-m)!}{(\ell+m)!}}\;\frac{P_\ell^m(\tanh\tau)}{\cosh^2\tau}\,,\qquad m=1,2,\dots\ell. \tag{3.70}$$

For $\nu^2>0$, the late time, $\tau\to\infty$, behaviour of the modes will be significant,

$$\mathcal{T}_\ell(\nu,\tau)\big|_{\tau\gg1}\to e^{-i\nu\tau}\,e^{-2\tau}, \tag{3.71}$$

as these modes are oscillatory. Applying infalling boundary conditions on these modes at the horizon of the topological AdS black hole, (3.66) yields,

$$F_\ell(\nu,z)=C_\ell(\nu)\,(1-z)^{-1-i\nu/2}\;{}_2F_1\left(-i\frac{\nu}{2},1-i\frac{\nu}{2};1-i\nu;1-z\right). \tag{3.72}$$

For the discrete series, the radial profile in the bulk, $F^{\rm N}_{\ell m}(z)$ is obtained by evaluating $F_\ell(\nu,z)$ at $\nu=-im$. Putting the above ingredients together, the general form of the electric field along the radial direction in the bulk is

$$\begin{aligned}A'_\tau(z,\tau,\theta)=\sum_{\ell=0}^{\infty}Y_\ell^0(\theta)\Bigg(\int_{-\infty}^{\infty}\frac{d\nu}{2\pi}\,\Gamma(1+i\nu)\,\frac{P_\ell^{-i\nu}(\tanh\tau)}{\cosh^2\tau}\;F_\ell(\nu,z)+\\+\sum_{m=1}^{\ell}\sqrt{m\frac{(\ell-m)!}{(\ell+m)!}}\,\frac{P_\ell^m(\tanh\tau)}{\cosh^2\tau}\,F^{\rm N}_{\ell m}(z)\Bigg).\end{aligned} \tag{3.73}$$

This also allows us to automatically solve for A'_θ using (3.65c) and we get

$$A'_\theta(z,\tau,\theta) = -\sum_{\ell=1}^{\infty} \frac{\partial_\theta Y^0_\ell(\theta)}{\ell(\ell+1)} \left(\int_{-\infty}^{\infty} \frac{d\nu}{2\pi}\, \Gamma(1+i\nu)\, \partial_\tau P_\ell^{-i\nu}(\tanh\tau)\; F_\ell(\nu,z) + \right. \\ \left. + \sum_{m=1}^{\ell} \sqrt{m\frac{(\ell-m)!}{(\ell+m)!}}\; \partial_\tau P_\ell^m(\tanh\tau)\, F^{\rm N}_{\ell\, m}(z) \right). \tag{3.74}$$

Now, the bulk gauge field action can be shown to induce a boundary term which will be the generating functional for the boundary R-current correlators. Using the explicit solutions above, the induced boundary action becomes

$$S = \frac{1}{2g^2_{\rm SG}} \int d\tau\; r_\chi \left[\sum_{\ell=0}^{\infty} \mathcal{F}_\ell(z,\tau)\, \mathcal{F}'_\ell(z,\tau) \cosh^2\tau + \sum_{\ell=1}^{\infty} \ell(\ell+1)\, \mathcal{G}_\ell(z,\tau)\, \mathcal{G}'_\ell(z,\tau) \right]_{z=\epsilon\to 0}. \tag{3.75}$$

The next step is to express this completely in terms of the boundary values of the gauge potentials $\mathcal{F}^0_\ell(\tau) \equiv \mathcal{F}_\ell(\epsilon,\tau)$ and $\mathcal{G}^0_\ell(\tau) \equiv \mathcal{G}_\ell(\epsilon,\tau)$. Their radial derivatives $\mathcal{F}_\ell{}'$ and $\mathcal{G}'_\ell$ (equivalently A'_τ and A'_θ) at the boundary $z=\epsilon$, are also determined completely by the boundary values of the gauge potentials, $\mathcal{F}^0_\ell(\tau)$ and $\mathcal{G}^0_\ell(\tau)$ as in (A.18).

From the boundary action above, we thus find that the real time, retarded Green's functions for the R-charge currents j^μ, in the gauge theory are

$$G^{\tau\tau}(\tau,\tau';\ell) = \ell(\ell+1)\left[\int_{-\infty}^{\infty} \frac{d\nu}{2\pi}\; \frac{\pi\nu}{\sinh\pi\nu}\; P_\ell^{-i\nu}(\tanh\tau) P_\ell^{i\nu}(\tanh\tau')\, \boldsymbol{\Upsilon}(\nu) + \right. \\ \left. + \sum_{m=1}^{\ell} (-1)^m\, m\, P_\ell^m(\tanh\tau) P_\ell^{-m}(\tanh\tau')\, \boldsymbol{\Upsilon}(i\,m) \right], \tag{3.76a}$$

$$G^{\theta\theta}(\tau,\tau';\ell) = \ell(\ell+1)\left[\int_{-\infty}^{\infty} \frac{d\nu}{2\pi}\; \frac{\pi\nu}{\sinh\pi\nu}\; \partial_\tau P_\ell^{-i\nu}(\tanh\tau)\, \partial_{\tau'} P_\ell^{i\nu}(\tanh\tau') \boldsymbol{\Upsilon}(\nu) + \right. \\ \left. + \sum_{m=1}^{\ell} (-1)^m\, m\, \partial_\tau P_\ell^m(\tanh\tau) \partial_{\tau'} P_\ell^{-m}(\tanh\tau')\, \boldsymbol{\Upsilon}(i\,m) \right], \tag{3.76b}$$

$$G^{\tau\theta}(\tau,\tau';\ell) = \ell(\ell+1)\left[\int_{-\infty}^{\infty} \frac{d\nu}{2\pi}\; \frac{\pi\nu}{\sinh\pi\nu}\; P_\ell^{-i\nu}(\tanh\tau)\, \partial_{\tau'} P_\ell^{i\nu}(\tanh\tau')\, \boldsymbol{\Upsilon}(\nu) + \right. \\ \left. + \sum_{m=1}^{\ell} (-1)^m\, m\, P_\ell^m(\tanh\tau) \partial_{\tau'} P_\ell^{-m}(\tanh\tau')\, \boldsymbol{\Upsilon}(i\,m) \right], \tag{3.76c}$$

$$\boldsymbol{\Upsilon}(\nu) = \frac{N^2 r_\chi}{64\pi^2 R_{\rm AdS}} \left(\psi\Big(-\frac{i\nu}{2} \Big) - \frac{1}{i\nu} \right). \tag{3.76d}$$

We need to first confirm that these Green functions satisfy basic consistency checks. Specifically, the retarded functions must vanish for $\tau < \tau'$. As in the previous case, this property is not manifest, but follows from the nature of the non-analyticities of $\boldsymbol{\Upsilon}(\nu)$, and the normalized mode functions $\Gamma(1+i\nu)P_\ell^{-i\nu}(\tanh\tau)$, in the complex ν-plane. For real values of ν, the associated Legendre function is [41, 42]

$$\Gamma(1+i\nu)\, P_\ell^{-i\nu}(\tanh\tau) = e^{-i\nu\tau}\, {}_2F_1(-\ell,\, \ell+1;\, 1+i\nu,\, (1-\tanh\tau)/2). \tag{3.77}$$

For integer ℓ, the hypergeometric function is a finite polynomial in $\tanh\tau$ and a ratio of degree ℓ polynomials of ν. Therefore the exponential frequency dependence means that, for $\tau - \tau' < 0$, the integrals over the frequency ν can be evaluated by closing the contour in the upper half plane. The function $\boldsymbol{\Upsilon}(\nu)$ has no poles in the upper half complex plane. It has simple poles at

$$\nu = 0,\ -2i,\ -4i \ldots \tag{3.78}$$

The normalized modes, $\Gamma(1+i\nu)P_\ell^{-i\nu}(\tanh\tau)$ have exactly ℓ simple poles in the upper half plane at $\nu = i, 2i \ldots \ell i$. The contributions from these are, however, cancelled by the inclusion of the discrete modes in the retarded Green's function above. Hence our correlators are zero for $\tau < \tau'$.

3.5.3 Late time behaviour

The real time response functions in general contain important information on the long time relaxation of perturbations away from the equilibrium or ground state. In thermal field theory on flat space, the relaxation of such fluctuations of conserved charges proceeds via hydrodynamic or diffusion modes. The response functions at strong coupling then exhibit diffusion poles in frequency space, $G^{\tau\tau} \propto (i\omega - Dk^2)^{-1}$, where ω is the frequency and k, the soft spatial momentum. Due to the explicit time dependence of the background metric, we cannot do a similar frequency space study of the full Green's functions in de Sitter space. Instead, we could analyze their behaviour as functions of time.

In de Sitter space, perturbations labelled by wave number ℓ, get red-shifted so that given sufficient time their physical wavelengths become super-horizon sized. This happens when

$$\frac{\ell\, e^{-\tau}}{R} \sim \frac{1}{R}. \tag{3.79}$$

At late enough times, even very high harmonics on the sphere get stretched and eventually exit the horizon. To zoom in on the time evolution of such modes, it is useful to think of $\ell e^{-\tau}$, the physical wave number, as being fixed as $\tau \to \infty$. For example, in this late time approximation we neglect terms like $\ell\, e^{-2\tau}$ in comparison to powers of $\ell\, e^{-\tau}$. This is practically equivalent to going to planar coordinates for de Sitter space and the mode functions behave as

$$P_\ell^{-i\nu}(\tanh\tau)\big|_{\ell e^{-\tau} = \text{fixed}} \longrightarrow \ell^{-i\nu}\, J_{i\nu}\left(2\ell e^{-\tau}\right) \tag{3.80}$$

It is possible to derive this by replacing the potential $\ell(\ell+1)\mathrm{sech}^2\tau$ in the mode equation (3.68), with $4\,\ell^2\, e^{-2\tau}$. Note that, instead of a fixed physical wavelength if we focus attention on fixed comoving wavenumber, given by ℓ, all modes simply approach the s-wave at late times,

$$\lim_{\tau\to\infty} \Gamma(1+i\nu)\, P_\ell^{-i\nu}(\tanh\tau)\big|_{\ell \text{ fixed}} \longrightarrow e^{-i\nu\tau}. \tag{3.81}$$

For fixed physical wavelengths, $\ell\, e^{-\tau}$, or equivalently, at the time when a harmonic ℓ crosses the horizon, the real time correlators are given by the exact results with the replacement (3.80). The integral over ν can be easily evaluated using the method of

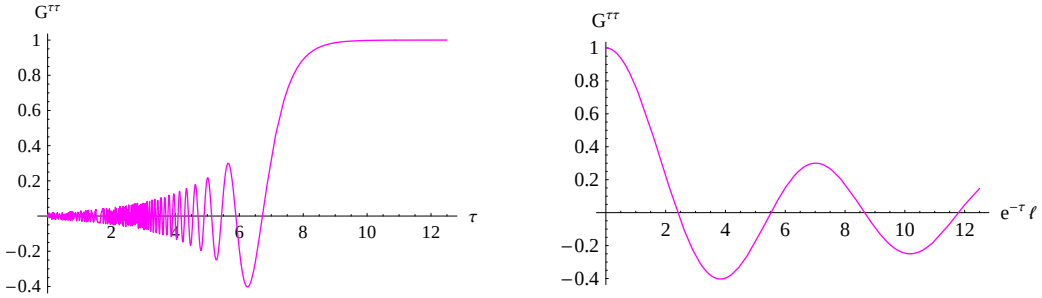

Figure 7. The leading behaviour of correlators $G_{\tau\tau}$ (and $G_{\tau\theta}$), up to normalization constants: as a function of τ on the left with $\ell = 1000$ and, on the right, as a function of $\ell e^{-\tau}$

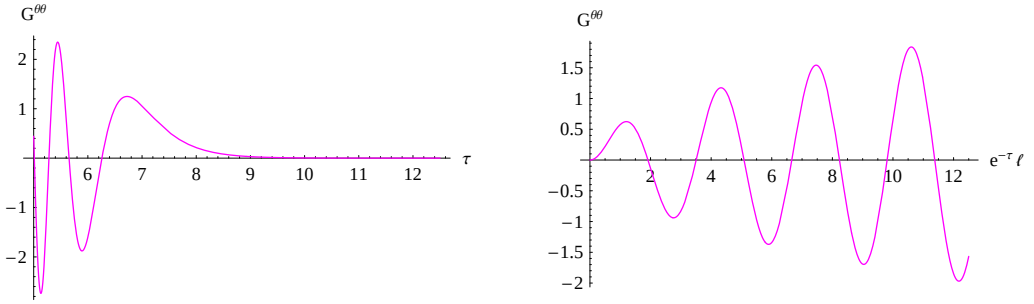

Figure 8. The leading behaviour of $G_{\theta\theta}$ (and $G_{\theta\tau}$): The left figure is plotted as a function of time for $\ell = 1000$, while the right hand side figure is a function of $\ell e^{-\tau}$.

residues, and it turns out that the leading contribution at late times is from the residue at $\nu = 0$. Thus

$$G^{\tau\tau}(\tau,\, 0; \ell),\;\; G^{\tau\theta}(\tau,\, 0; \ell) \;\sim\; J_0(2\,\ell e^{-\tau}) \tag{3.82}$$

and

$$G^{\theta\tau}(\tau, 0;\, \ell),\;\; G^{\theta\theta}(\tau, 0;\, \ell) \;\sim\; \partial_\tau J_0(2\,\ell e^{-\tau}). \tag{3.83}$$

This late time behaviour is depicted in figures 7 and 8.

The late time behaviour deduced above is not characteristic of diffusion in de Sitter space. Suppose that the R-charge fluctuation relaxed via diffusion modes, then the covariant conservation of the R-current together with Fick's law would lead to the diffusion equation

$$\partial_\tau j^\tau = D\nabla_\theta\nabla^\theta\, j^\tau, \tag{3.84}$$

in dS_3, D being the diffusion constant. The spherical harmonics of j^τ on the expanding spatial spherical sections would then obey,

$$\partial_\tau j^\tau_\ell = -D\,\frac{\ell(\ell+1)}{\cosh^2\tau}\, j^\tau_\ell\,. \tag{3.85}$$

At late times $\tau \to \infty$ and large enough ℓ, this is solved by

$$j^\tau_\ell \sim \exp\left(\frac{1}{2} D\,\ell^2\, e^{-2\tau}\right). \tag{3.86}$$

JHEP04(2009)063

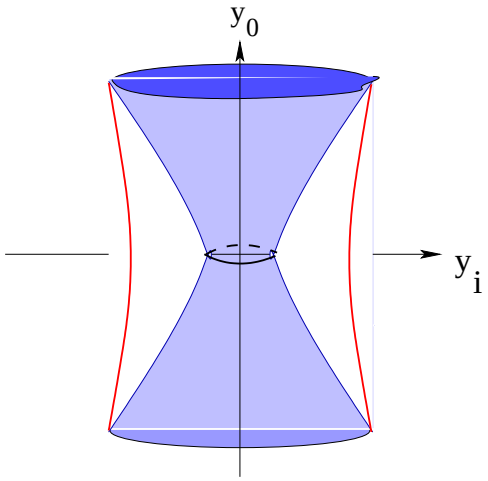

Figure 9. The global structure of the bubble geometry. The region inside the shaded region is empty, and its surface represents the de Sitter expansion of the bubble at $r = r_h$.

The large time behaviour of the Green's functions (3.82) and (3.83) do not match up with expected diffusive relaxation (3.86) on dS_3. A natural reason for this is that the rate of exponential expansion of the spatial section and the Gibbons-Hawking temperature are both set by R^{-1}. Thus the mean free path or the mean free time between collisions is comparable to the expansion time scales so that the system never enters a diffusive regime.

4 The (small) AdS bubble of nothing

The topological AdS black hole discussed above has a semiclassical instability when

$$r_\chi < \frac{R_{\rm AdS}}{2\sqrt{2}} \tag{4.1}$$

which causes it to decay into a "bubble of nothing" in AdS space. The instability only occurs if fermions have antiperiodic boundary conditions in the χ-direction. With periodic boundary conditions for both bosons and fermions, the topological AdS black hole is absolutely stable.

As originally pointed out in [9] (and [7] in the present context), the decay of a false vacuum in semiclassical gravity is computed by the Euclidean bounce which has the same asymptotics as the false vacuum in Euclidean signature. The bounce is a solution to the Euclidean equations of motion with a non-conformal negative mode. In the context of the asymptotically (locally) AdS spaces in question, the small Euclidean Schwarzschild solution represents such a bounce solution. In Lorentzian signature, the semiclassical picture of the decay process at time $t = 0$ (say) involves replacing the $t > 0$ part of the false vacuum solution (the topological black hole) with the appropriate analytic continuation of the Euclidean bounce to Lorentzian signature. The analytic continuation of the small Euclidean AdS black hole bounce which leads to $dS_3 \times S^1$ boundary asymptotics, is the (small) AdS

JHEP04(2009)063

bubble-of-nothing. The metric for the AdS bubble-of-nothing solution is

$$ds^2 = f(r)\, r_\chi^2\, d\chi^2 + f(r)^{-1}\, dr^2 + r^2 \left(-\frac{dt^2}{R_{\mathrm{AdS}^2}} + \cosh^2\left(\frac{t}{R_{\mathrm{AdS}}}\right) d\Omega_2^2 \right),$$
$$f(r) = 1 + \frac{r^2}{R_{\mathrm{AdS}}^2} - \frac{r_h^2 (R_{\mathrm{AdS}}^2 + r_h^2)}{r^2}. \tag{4.2}$$

In order to avoid a conical singularity in the interior, the periodicity of the compact χ coordinate is related to r_h as

$$2\pi r_\chi = 2\pi R_{\mathrm{AdS}}^2\, \frac{r_h}{r_h^2 + R_{\mathrm{AdS}}^2}. \tag{4.3}$$

Passing to the dimensionless coordinates introduced earlier,

$$\rho = \sqrt{(r/R_{\mathrm{AdS}})^2 + 1}, \qquad \tau = \frac{t}{R_{\mathrm{AdS}}}, \qquad \tilde{r}_h = \frac{r_h}{R_{\mathrm{AdS}}}, \tag{4.4}$$

the metric becomes

$$ds^2 = R_{\mathrm{AdS}}^2 \left[\tilde{f}(\rho)\, \frac{r_\chi^2}{R_{\mathrm{AdS}}^2}\, d\chi^2 + \tilde{f}(\rho)^{-1}\, \frac{\rho^2}{\rho^2 - 1}\, d\rho^2 + (\rho^2 - 1)(-d\tau^2 + \cosh^2\tau d\Omega_2^2) \right] \tag{4.5a}$$
$$\tilde{f}(\rho) = \rho^2 - \frac{1}{\rho^2 - 1}\, \tilde{r}_h^2\, \left(\tilde{r}_h^2 + 1\right). \tag{4.5b}$$

In the AdS bubble of nothing spacetime, a slice of constant ρ is $dS_3 \times S^1$. The S^1, however, shrinks to zero size smoothly at $\rho = \sqrt{\tilde{r}_h^2 + 1}$. The shrinking circle is the cigar of the Euclidean Schwarzschild solution. The boundary of the spacetime is approached as $\rho \to \infty$. The semiclassical decay of the topological black hole at $\tau = 0$, results in the sudden appearance of a bubble of nothing in the region of spacetime, $\rho^2 \leq 1 + \tilde{r}_h^2$.

4.1 WKB for the AdS bubble of nothing

An exact holographic computation of correlation functions in the AdS bubble of nothing background appears difficult as analytical solutions to the wave equation in this background are not known. Despite this, we may obtain the boundary Green's function following a systematic approximation. In particular we will employ the WKB approximation to determine boundary correlation functions at high frequency and large mass. The WKB approximation has been used successfully [39] to find high frequency Green's functions in the Big AdS-Schwarzschild black hole. In this approximation, lines of isolated singularities (poles) get replaced by branch cuts since, in the high frequency regime, the separation between poles effectively goes to zero, as seen in our example above in section 2.3.1.

We first take the massive scalar wave equation

$$\frac{1}{\sqrt{-g}}\, \partial_\mu (g^{\mu\nu} \sqrt{-g}\, \partial_\nu \Phi) - M^2 \Phi = 0, \tag{4.6}$$

in the bubble background and expand the scalar field in harmonics on $dS_3 \times S^1$ as in (3.3). The harmonics $\Phi_n(\nu, \rho)$ then satisfy a radial differential equation which can be put in the

form

$$\frac{d^2\Phi_n}{dx^2}+\left(\frac{1}{x-1}+\frac{1}{x+\tilde{r}_h^2}+\frac{1}{x-\tilde{r}_h^2-1}\right)\frac{d\Phi_n}{dx}+\frac{1}{4(x-1)(x+\tilde{r}_h^2)(x-\tilde{r}_h^2-1)}\times \\ \times\left(\nu^2+1-n^2\frac{R_{\rm AdS}^2}{r_\chi^2}\frac{(x-1)^2}{(x+\tilde{r}_h^2)(x-\tilde{r}_h^2-1)}-M^2R^2(x-1)\right)\Phi_n=0, \tag{4.7}$$

where $x=\rho^2$ and n labels the momentum along the S^1. This is an ordinary differential equation with four regular or nonessential singular points at $x=1$, $-\tilde{r}_h^2$, $\tilde{r}_h^2+1$ and ∞. Analytical solutions for this type of equation are unknown. In fact, a similar differential equation was encountered in the computation of glueball masses at strong coupling in the three dimensional effective theory obtained from Euclidean thermal $\mathcal{N}=4$ SYM [40] (on $\mathbb{R}^3\times S^1$ with SUSY-breaking boundary conditions). In that case the dual bulk geometry is the Euclidean black brane solution in AdS space where the thermal circle shrinks to zero size smoothly.

The WKB solutions to the wave equation can be found after going to the Schrödinger form by introducing the variables

$$\Phi=\frac{\Psi}{\sqrt{\rho(\rho^2-1)}}, \tag{4.8a}$$

$$u=\frac{\tilde{r}_h}{1+2\tilde{r}_h^2}\,\cot^{-1}\left(\frac{\rho}{\tilde{r}_h}\right)+\frac{\sqrt{1+\tilde{r}_h^2}}{1+2\tilde{r}_h^2}\,\coth^{-1}\left(\frac{\rho}{\sqrt{1+\tilde{r}_h^2}}\right). \tag{4.8b}$$

These are the natural generalizations of (3.6) and (3.7) to the bubble of nothing geometry. The cigar in the geometry gets smoothly capped off at $\rho=\sqrt{\tilde{r}_h^2+1}$, where the spacetime ends. In terms of the u coordinate, this occurs as $u\to\infty$. In terms of the harmonics of Ψ on the $dS^3\times S^1$ slices, as in (3.3), we obtain the Schrödinger equation obeyed by the harmonics $\Psi_n(\nu,u)$ in the (small) AdS bubble of nothing:

$$-\frac{d^2}{du^2}\,\Psi_n(\nu,u)+\tilde{V}_n(\nu,u)\,\Psi_n(\nu,u)=0, \tag{4.9a}$$

$$\tilde{V}_n(\nu,u)=\left((MR)^2-\frac{\nu^2+1}{\rho^2-1}\right)\left(\rho^2-1-\frac{1}{\rho^2}\,\tilde{r}_h^2\,(\tilde{r}_h^2+1)\right)+ \\ +n^2\frac{R_{\rm AdS}^2}{r_\chi^2}\,\frac{\rho^2-1}{\rho^2}+\frac{1}{4\rho^2}\,(15\rho^4-10\rho^2-1). \tag{4.9b}$$

Here ρ is implicitly a function of u, determined by the solution to (4.8b). In addition to the fact that the Schrödinger potential is far more complicated than (3.9), one crucial difference to the TBH case is that the potential cannot be defined independent of the frequency itself. This is due to the term proportional to $\tilde{r}_h$ in (4.9b). This situation is also in contrast to the case of the big AdS-Schwarzschild black hole in [39]. Here, for a given frequency (and mass), we need to find the "zero energy" eigenstate of the Schrödinger problem (4.9a).

Interestingly, the qualitative behaviour of the potential $\tilde{V}_n$ changes, depending on the relative values of the mass and the frequency. This is illustrated in figures 10 and 11.

JHEP04(2009)063

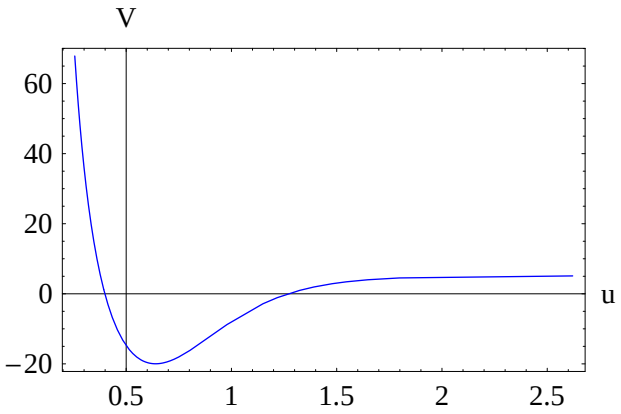

Figure 10. The Schrödinger potential for a massive scalar in the AdS bubble of nothing. In the above plot the dimensionless frequency $\nu = 7$, the mass $MR = 2$ and $\tilde{r}_h = r_h/R_{\rm AdS} = 1$.

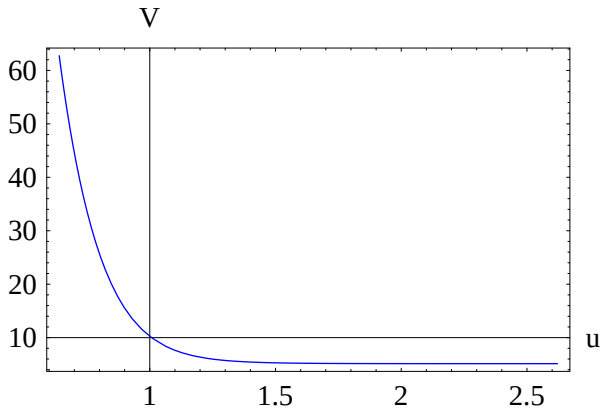

Figure 11. The Schrödinger potential for $\nu = 7$, the mass $MR = 7$ and $\tilde{r}_h = r_h/R_{\rm AdS} = 1$.

The qualitative nature of the potential is easy to grasp in the high frequency limit, wherein we take

$$\nu \to \infty, \quad MR \to \infty, \quad \tilde{\nu} = \frac{\nu}{MR} \text{ fixed.} \tag{4.10}$$

For simplicity, we also set $n = 0$, focussing attention on the spatially homogeneous fields. In this approximation,

$$\tilde{V}_0(\nu, u) \to \mathcal{V}(\tilde{\nu}, u) = (MR)^2 \left(1 - \frac{\tilde{\nu}^2}{\rho^2 - 1}\right) \left(\rho^2 - 1 - \frac{1}{\rho^2}\, \tilde{r}_h^2(\tilde{r}_h^2 + 1)\right). \tag{4.11}$$

The potential is vanishing (having thrown away a subleading constant in the large frequency limit) at the tip of the cigar $\rho = \sqrt{\tilde{r}_h^2 + 1}$. Using $u \sim -\ln(\rho - \sqrt{\tilde{r}_h^2 + 1})$ near this point, it follows that $\mathcal{V}(\tilde{\nu}, u)$ decays exponentially as a function of u. The potential has another zero at $\rho = \sqrt{\tilde{\nu}^2 + 1}$. Now, since the spacetime ends at $\rho = \sqrt{1 + \tilde{r}_h^2}$, the number of zeroes of the potential depends on whether $|\tilde{\nu}|$ is greater than or less than $\tilde{r}_h$. In particular, when $|\tilde{\nu}| > \tilde{r}_h$, the potential energy has two zeroes or turning points, and qualitatively resembles figure 10, while for $|\tilde{\nu}| < \tilde{r}_h$, it behaves as in figure 11 (the potential asymptotes to a

JHEP04(2009)063

constant different from zero in the figures; however this constant becomes negligible in the high frequency limit).

Zero energy Schrödinger wave functions in the potential (4.11) are marginally bound states for $|\tilde{\nu}| > \tilde{r}_h$, since the potential has two turning points. For $|\tilde{\nu}| < \tilde{r}_h$, there is only one turning point and the wave function should exhibit a qualitative change in its behaviour at $|\tilde{\nu}| = \tilde{r}_h$. This also strongly suggests that in the complex frequency plane, $\tilde{\nu} = \pm\tilde{r}_h$ should be singularities of boundary correlation functions.

The zero energy wave function for the Schrödinger equation can be obtained in the WKB approximation, where care needs to be taken in applying the matching conditions at each of the turning points in the potential. We treat the two cases $|\tilde{\nu}| > \tilde{r}_h$ and $|\tilde{\nu}| < \tilde{r}_h$ separately.

WKB approximation for $\tilde{\nu}^2 > \tilde{r}_h^2$. There are two distinct regions in the potential: (i) the "quantum tunnelling region", $\sqrt{1+\tilde{\nu}^2} < \rho < \infty$ which we label as Region I, and (ii) the "propagating region", $\sqrt{1+\tilde{r}_h^2} < \rho < \sqrt{1+\tilde{\nu}^2}$ which we call Region II.

In Region I, we write the WKB solutions as

$$\Psi_{\rm WKB}(\tilde{\nu}, u) = \frac{1}{\mathcal{V}^{1/4}} \left(A_+ \exp\left(\int_{u_c}^{u} \sqrt{\mathcal{V}}\, du \right) + A_- \exp\left(-\int_{u_c}^{u} \sqrt{\mathcal{V}}\, du \right) \right). \tag{4.12}$$

where the classical turning point u_c is defined by

$$\rho(u_c) \equiv \sqrt{\tilde{\nu}^2 + 1}. \tag{4.13}$$

These represent the growing and decaying modes in the near boundary region of the bulk geometry. This can be understood easily as follows.

$$\left.\frac{du}{d\rho}\right|_{\rho\to\infty} \approx -\frac{1}{\rho^2} \quad \Longrightarrow \mathcal{V} \approx (MR)^2\, \rho^2 \tag{4.14}$$

which then immediately yields the near boundary WKB solution (4.12) for Ψ. This together with its relation (4.8b) to the massive bulk scalar field Φ implies

$$\Phi_{\rm WKB}\big|_{\rho\to\infty} \sim A_+ \,(\cdots)\rho^{-2-MR} + A_- \,(\cdots)\,\rho^{-2+MR} \tag{4.15}$$

where the ellipses denote unspecified normalization constants. The two power laws appearing in this solution are precisely the normalizable and non-normalizable modes of the massive scalar field, in the limit of large mass, in an asymptotically (locally) AdS spacetime. Following the prescription for computing the retarded Green's functions, we normalize $\Psi_{\rm WKB}$ (4.15) so that it approaches unity near the boundary.

In the interior, however, for $\rho \le \sqrt{1+\tilde{\nu}^2}$ the solutions enter Region II and become oscillatory. In Region II, we have

$$\Psi_{\rm WKB}(\tilde{\nu}, u) = \frac{1}{|\mathcal{V}|^{1/4}} \left(B_+ \exp\left(i\int_{u_c}^{u} \sqrt{|\mathcal{V}|}\, d\rho \right) + B_- \exp\left(-i\int_{u_c}^{u} \sqrt{|\mathcal{V}|}\, du \right) \right). \tag{4.16}$$

The constants are uniquely determined by the WKB matching conditions at the classical turning points of the potential $\mathcal{V}(\tilde{\nu}, u)$ and the one normalization condition on A_- near the

JHEP04(2009)063

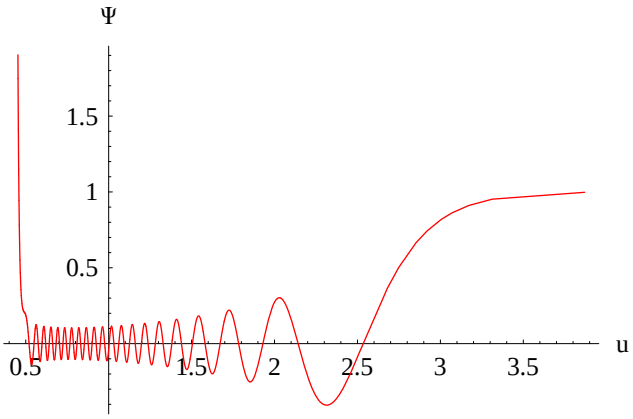

Figure 12. The exact numerical solution to the Schrödinger problem for the AdS bubble of nothing. Here $\nu R = 200$, $MR = 100$ and $r_h/R = 1$. The solution approaches a constant for $u \gg 1$, while the classically forbidden region is $0 < u < u_c \approx 0.49$.

boundary. The details of the WKB matching conditions are explained in appendix B. The crucial result of the matching procedure is that the solution in the near boundary region (Region I) has a normalizable mode with strength

$$A_+ = -\frac{1}{2} A_- \ \tan\left(\int_\infty^{u_c} \sqrt{|\mathcal{V}(\tilde{\nu}, u)|} du\right) \tag{4.17}$$

The argument in the above expession can, as usual, be identified with the action of a zero energy classical particle trapped in the potential $\mathcal{V}(\tilde{\nu}, u)$ between the two turning points u_c and $u \to \infty$ (the latter corresponding to $\rho \to \sqrt{1 + \tilde{r}_h^2}$ where spacetime ends).

The crucial difference between the bubble of nothing geometry and the topological black hole is the boundary condition imposed on the solutions to the wave equation in the interior. To extract retarded correlators from the geometry with a horizon we impose an infalling condition on the plane wave solutions near the horizon. In the bubble geometry, however, since spacetime ends smoothly in the interior where the cigar caps off, there is no freedom in choosing the boundary condition at the tip of the cigar – we must require regularity (normalizability) of solutions in the interior. This means that the solution to the Schrödinger equation (4.9a) must approach a constant exponentially as $u \to \infty$.

The Green's function at high frequency is completely determined (up to contact terms) by the ratio A_+/A_-. After substituting the solution (4.15) into the boundary action we find,

$$\tilde{G}_R(\tilde{\nu}) \approx \lim_{\epsilon \to 0} MR \ \exp\left(2\int_{u_c}^{\epsilon} \sqrt{\mathcal{V}(\tilde{\nu}, u)}\, du\right) \ \tan\left(\int_\infty^{u_c} \sqrt{|\mathcal{V}(\tilde{\nu}, u)|}\, du\right). \tag{4.18}$$

The exponential prefactor in this expression is the WKB transmission coefficient into the classically forbidden Region I. The physically relevant contribution to the transmission coefficient is the constant, ϵ-independent term in an expansion around the boundary $\epsilon \to 0$. The leading ϵ dependence, which is an overall multiplicative constant proportional to ϵ^{2MR}, can be absorbed into the normalization of the correlation function.

JHEP04(2009)063

The first observation we can make without actually evaluating (4.18), is that it has an infinite set of poles as a function of $\tilde{\nu}$ on the real axis for $\tilde{\nu}^2 > r_h^2$. These occur whenever

$$\mathcal{S}_{\rm II}(\tilde{\nu},\ MR) = \int_{\infty}^{u_c} du\sqrt{|\mathcal{V}(\tilde{\nu},u)|} = \left(n+\frac{1}{2}\right)\pi\,, \quad n\in\mathbb{Z}. \tag{4.19}$$

That is, the semiclassical action in the propagating region is a half-integral multiple of π. This is of course the condition for the existence of a bound state wave function, and the poles in the Green's function reflect the appearance of these bound states at certain values of $\tilde{\nu}$ on the real axis. Recall that the corresponding correlators in the topological black hole phase do not have any poles on the real axis.

At first sight the poles on the real frequency axis might appear somewhat surprising. However, they have the following natural physical interpretation: the low energy physics of the gauge theory on the boundary of the AdS bubble of nothing is that of nonsupersymmetric Yang-Mills theory at large N (and strong 't Hooft coupling) on dS_3. The antiperiodic boundary conditions on the spatial S^1 make all fermionic excitations massive and the broken supersymmetry leads to large radiative corrections to the scalar masses. In the strongly coupled theory, the dynamical scale of the three dimensional effective theory is expected to be set by r_χ^{-1}, the scale of the compact S^1 direction. When the Gibbons-Hawking temperature $T_H = 1/(2\pi R)$ in dS_3 is smaller than r_χ^{-1}, we expect the gauge theory to be in a confined phase where the degrees of freedom are gauge singlet glueballs. The appearance of the isolated poles in the high frequency correlators is consistent with this physical picture.

The WKB integral in Region II, in the high frequency approximation to the Green's function (4.18) can be expressed in terms of complete elliptic integrals as

$$\begin{aligned}
\mathcal{S}_{\rm II}(\tilde{\nu},\ MR) &= \frac{1}{2}MR\int_{\tilde{\nu}^2+1}^{\tilde{r}_h^2+1} dx\ \frac{\sqrt{\frac{\tilde{\nu}^2}{x-1}-1}}{\sqrt{(x+\tilde{r}_h^2)(x-\tilde{r}_h^2-1)}} \\
&= i\,\frac{MR}{\sqrt{1+2\tilde{r}_h^2}}\left[|\tilde{\nu}|\left(K\left(\frac{a}{b}\right)-\sqrt{\frac{b}{a}}\,K\left(\frac{b}{a}\right)\right)\right. \\
&\qquad\qquad \left. +\frac{1}{|\tilde{\nu}|}(1+\tilde{r}_h^2)\left(\Pi\left(a|\frac{a}{b}\right)-\sqrt{\frac{b}{a}}\,\Pi\left(b|\frac{b}{a}\right)\right)\right], \\
a &= \frac{\tilde{\nu}^2+1+\tilde{r}_h^2}{\tilde{\nu}^2}\,, \\
b &= \frac{1+2\tilde{r}_h^2}{\tilde{r}_h^2}\,, \qquad \tilde{\nu}^2 > r_h^2.
\end{aligned} \tag{4.20}$$

From the general characteristics of these elliptic functions and their singularities [41], it can be checked that $\mathcal{S}_{\rm II}(\tilde{\nu},\ MR)$ has no singularities on the real axis for $\tilde{\nu}^2 > \tilde{r}_h^2$. Potential logarithmic branch points at $\tilde{\nu}^2 = \tilde{r}_h^2$ and at $\tilde{\nu} = 0$, cancel out between the individual terms above. In fact, for any fixed value of $\tilde{r}_h$, it also follows that, for large $\tilde{\nu}$, the WKB integral increases linearly with $\tilde{\nu}$.

$$\mathcal{S}_{\rm II} \propto |\tilde{\nu}|\,; \qquad |\tilde{\nu}| \gg 1. \tag{4.21}$$

JHEP04(2009)063

Hence for $|\tilde{\nu}| \gg \tilde{r}_h$, the propagator (4.18) has approximately equally spaced simple poles on the real axis, whenever $\mathcal{S}_{\rm II} = (n + \frac{1}{2})\pi$.

Although there are no other sources of singularities from $S_{\rm II}$, the WKB transmission coefficient in Region I, which also enters the Green's function (4.18) can have branch point singularities on the real axis,

$$\mathcal{S}_I(\tilde{\nu},\ MR) = -\frac{1}{2}MR\int_{1+\tilde{\nu}^2}^{1/\epsilon^2} dx \frac{\sqrt{1-\frac{\tilde{\nu}^2}{x-1}}}{\sqrt{(x+\tilde{r}_h^2)(x-\tilde{r}_h^2-1)}}$$

$$= -\frac{MR}{\sqrt{1+2\tilde{r}_h^2}}\left(|\tilde{\nu}|\left(F\left(\csc^{-1}\sqrt{a},\ \frac{a}{b}\right) - K\left(\frac{a}{b}\right)\right) - \frac{1}{|\tilde{\nu}|}(1+\tilde{r}_h^2)\,\Pi\left(a|\frac{a}{b}\right)\right) \tag{4.22}$$

$$-\frac{1}{2}MR\left(\ln\left(\frac{2\epsilon^{-2}}{|\tilde{\nu}|\sqrt{1+\tilde{r}_h^2}}\right) + i\pi\right).$$

This function is also free of any branch cuts at $\tilde{\nu} = \pm\tilde{r}_h$, as can be checked by directly evaluating the integral at this point. However, the logarithmic growth at large $\tilde{\nu}$ implies a branch point at infinity.

As an aside we mention that the high frequency limit in the topological black hole phase (3.40) can be rederived by formally setting $\tilde{r}_h = 0$ in the WKB integrals and $\tilde{G}_R(\tilde{\nu}) \sim \exp(2\,\mathcal{S}_I)$.

WKB for $\tilde{\nu}^2 < \tilde{r}_h^2$. For low (real) frequencies $\tilde{\nu}^2 < \tilde{r}_h^2$, the nature of the WKB potential changes (figure 11). Bound states are no longer possible. The zero energy WKB solution is

$$\Psi_{\rm WKB}(\tilde{\nu}, u) = A_+\,\frac{1}{\mathcal{V}^{1/4}}\,\exp\left(\int_\infty^u \sqrt{\mathcal{V}}\,du\right) + A_-\frac{1}{\mathcal{V}^{1/4}}\exp\left(-\int_\infty^u \sqrt{\mathcal{V}}\,du\right). \tag{4.23}$$

The relation between the two coefficients is determined by matching to the wavefunction at large u, where the potential decays exponentially and the wavefunction is a modified Bessel function (see appendix B). We find that

$$A_+ = iA_-. \tag{4.24}$$

The aymptotics of this solution near the boundary at $u = \epsilon$ (B.25) allows to compute the boundary action and the Green's function

$$\tilde{G}_R(\tilde{\nu}) \approx \lim_{\epsilon\to 0} i\,MR\,\exp(\mathcal{S}_I) = i\,MR\,\exp\left(2\int_\infty^\epsilon \sqrt{\mathcal{V}(\tilde{\nu},u)}\,du\right). \tag{4.25}$$

In terms of elliptic functions the explicit form for the WKB action is

$$\mathcal{S}_I = -\frac{MR}{\sqrt{1+2\tilde{r}_h^2}}\left(|\tilde{\nu}|(F\left(\csc^{-1}\sqrt{a},\ \frac{a}{b}\right) - \sqrt{\frac{b}{a}}K\left(\frac{b}{a}\right) - \frac{1}{|\tilde{\nu}|}(1+\tilde{r}_h^2)\sqrt{\frac{b}{a}}\Pi\left(a|\frac{b}{a}\right)\right)$$

$$-\frac{1}{2}MR\left(\ln\left(\frac{2\epsilon^{-2}}{|\tilde{\nu}|\sqrt{1+\tilde{r}_h^2}}\right) + i\,\pi\right), \tag{4.26}$$

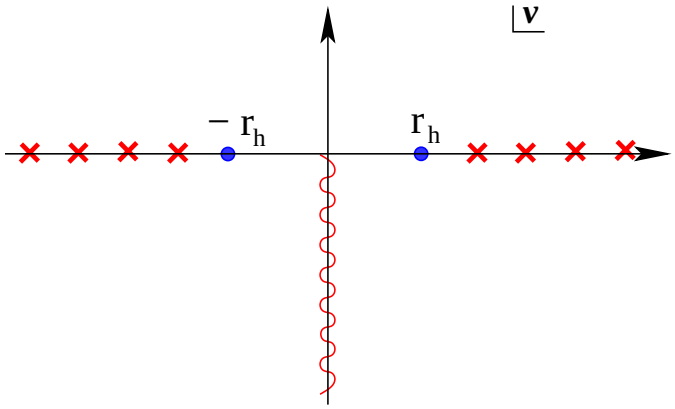

Figure 13. The analytic structure of the boundary Green's function in the " bubble of nothing" phase in the WKB approximation $\nu \to \infty$, $MR \to \infty$ with $\tilde{\nu} = \nu/MR$ fixed. Approximately equally spaced simple poles on the real axis for $\tilde{\nu}^2 > \tilde{r}_h^2$, are accompanied by branch points at $\tilde{\nu} = 0$ and infinity.

and the only singularity of this expression is the logarithmic singularity at $\tilde{\nu} = 0$ which complements the singularity at $\tilde{\nu} = \infty$ found above.

The resulting analytic structure of the Green's function is summarized in figure 13, which is to be contrasted with corresponding Green's function (at large mass and frequency) in the topological black hole phase in figure 6. As already dicussed earlier, the isolated poles on the real axis indicate glueball states and that the gauge theory is in the confined phase, wherein the radius of the spatial S^1 is much smaller than the dS_3 radius of curvature. This may be interpreted as a hadronized phase, the de Sitter temperature being too low for the degrees of freedom to be deconfined. In this context, we should point out that the high frequency WKB analysis, where the frequencies are much larger than the de Sitter cosmological constant, is basically a flat space limit and thus the singularities of the Green's functions may be interpreted in the standard way as in flat space. One feature of the propagator in the bubble-of-nothing phase whose origin is not entirely clear is the branch point singularity at $\tilde{\nu} = 0$. A similar branch point at $\tilde{\nu} = -i$ was encountered in the high frequency limit in the topological black hole phase. The associated branch cut was a consequence of the apparent merger of the infinite set of quasinormal poles of the topological black hole, in the high frequency limit. We do not know of a similar interpretation of the branch cuts of (4.26) and figure 13.

5 Summary and discussion

In this paper, we have studied real time correlators in strongly coupled $\mathcal{N} = 4$ SUSY Yang-Mills theory on a time-dependent background, namely $dS_3 \times S^1$. In particular, we have calculated the retarded scalar glueball correlators and the R-charge current correlators in the $\mathbb{Z}_N$-invariant phase.

The retarded scalar glueball correlators have an infinite number of poles in the lower half of the complex frequency plane, which represent the topological black hole quasinor-

JHEP04(2009)063

mal frequencies. The imaginary parts of these correlators are associated to the Gibbons-Hawking temperature due to the cosmological horizon of dS_3. These two facts suggest that the $\mathbb{Z}_N$ symmetric phase of the boundary field theory corresponds to a deconfined plasma in the exponentially expanding universe.

We also computed the retarded correlators for the spatial spherical harmonics of the conserved R-currents using the Son-Starinets approach. Here we encountered a subtle point wherein we had to include in our mode expansions, the effects of real, normalizable, discrete solutions to the de Sitter mode equations, in order to obtained a retarded Green's function. The corresponding frequency space correlator, appropriately defined in de Sitter space, also has an infinite number of poles in the lower half of the complex frequency plane, but these do not appear to correspond to diffusive poles. The lack of hydrodynamic behavior of the system is presumably due to the fact that the expansion rate of dS_3 is of the same order as the Gibbons-Hawking temperature. Here, we did not calculate the correlators of the stress-energy tensor. However, using the same argument as above, we expect not to find any hydrodynamic poles there either.

In this paper, we have also calculated the retarded correlators of scalar operators $\mathcal{O}_\Delta$, with conformal dimension $\Delta \gg 1$, in both the $\mathbb{Z}_N$-invariant phase and $\mathbb{Z}_N$ broken bubble phase. Unlike the correlators of the $\mathbb{Z}_N$ symmetric phase, the correlators in the $\mathbb{Z}_N$ broken phase feature an infinite number of poles on the real frequency axis. These poles are naturally associated to bound glueball-like states, which suggests that this phase is a hadronized phase, where the de Sitter temperature is too low to deconfine the degrees of freedom (the Hubble parameter is low compared to the dynamical scale of the effective, non-SUSY 3d theory on dS_3). Since this geometry contains no horizon, Son-Starinets prescription [27] is not applicable in this phase and we have restricted ourselves to the high frequency and large mass regime by using WKB approximation. Since the prescription proposed by Skenderis and van Rees [25, 26] does not rely on the existence of horizons in the geometry, it would be interesting to see whether one can obtain the retarded correlators beyond the high frequency limit using this prescription.

It is also interesting to note that the relevant boundary condition on the horizon as prescribed by Son and Starinets [27] implies that the boundary theory is in the Euclidean or Bunch-Davies vacuum. This is in agreement with ref. [6], where it was argued that due to the fact that the α-vacua Wightman functions for the topological black hole develop singularities on the event horizon, the preferred vacuum for the boundary field theory is the Bunch-Davis vacuum. It would be interesting to see whether one can understand the issue of α-vacua ambiguity better by applying the Skenderis-van Rees prescription [25, 26] to this set-up.

Acknowledgments

The authors would like to thank Carlos Hoyos, Asad Naqvi, Simon Ross and Kostas Skenderis for useful discussions. J. H. is supported by the De Benedetti Family Fellowship in Physics and in part by DOE grant DE-FG03-91-ER40682. J.R. is supported by an STFC studentship.

JHEP04(2009)063

A Boundary action for bulk Maxwell fields

A.1 Nonvanishing S^1 momentum

We provide here, the steps in the calculation leading to the boundary action for fluctuations which are homogeneous on the spatial slices of dS_3 but with momentum along the spatial S^1. The equations of motion (3.55a),(3.55b) can be solved in terms of hypergeometric functions

$$\mathcal{F}'_n = C_\tau(\nu,\bar{n})\ (1-z)^{-i(\nu-i)/2}\ {}_2F_1\left(\frac{1}{2}+\frac{i}{2}(\bar{n}-\nu)\,,\frac{1}{2}-\frac{i}{2}(\bar{n}+\nu)\,;1-i\nu\,;1-z\right). \tag{A.1}$$

Here C_τ is a frequency dependent constant, to be determined by the boundary values of the fields. Near the boundary of AdS space, the solution approaches

$$\begin{aligned}\mathcal{F}'_n\big|_{z\to 0} =-\ C_\tau\ &\frac{\Gamma(1-i\nu)}{\Gamma\left(\frac{1}{2}+\frac{i}{2}(\bar{n}-\nu)\right)\Gamma\left(\frac{1}{2}-\frac{i}{2}(\bar{n}+\nu)\right)}\times\\ &\times\left(2\gamma_E+\ln z+\psi\left(\frac{1}{2}+\frac{i}{2}(\bar{n}-\nu)\right)+\psi\left(\frac{1}{2}-\frac{i}{2}(\bar{n}+\nu)\right)\right).\end{aligned} \tag{A.2}$$

Imposing the boundary conditions at $z\to 0$

$$\lim_{\epsilon\to 0}\mathcal{F}_n(\nu,\epsilon)=\mathcal{F}^0_n(\nu),\qquad \lim_{\epsilon\to 0}\mathcal{G}_n(\nu,\epsilon)=\mathcal{G}^0_n(\nu), \tag{A.3}$$

from (3.54b) we find that

$$C_\tau(\nu,\bar{n})=-\frac{\Gamma\left(\frac{1}{2}+\frac{i}{2}(\bar{n}-\nu)\right)\Gamma\left(\frac{1}{2}-\frac{i}{2}(\bar{n}+\nu)\right)}{4\Gamma(1-i\nu)}\ \left(\bar{n}^2\mathcal{F}^0_n(\nu)-\frac{R_{\rm Ads}}{r_\chi}\,\bar{n}(\nu-i)\,\mathcal{G}^0_n(\nu)\right). \tag{A.4}$$

With the normalization fixed in terms of the boundary values of the relevant fields we have that

$$\begin{aligned}\mathcal{F}'_n(\nu,\epsilon)=&\frac{1}{4}\left(\bar{n}^2\mathcal{F}^0_n-\frac{R_{\rm AdS}}{r_\chi}\,\bar{n}(\nu-i)\mathcal{G}^0_n\right)\ \times\\ &\left(2\gamma_E+\ln\epsilon+\psi\left(\frac{1}{2}+\frac{i}{2}(\bar{n}-\nu)\right)+\psi\left(\frac{1}{2}-\frac{i}{2}(\bar{n}+\nu)\right)\right).\end{aligned} \tag{A.5}$$

From (3.54a) we also obtain

$$\mathcal{G}'_n(\nu,\epsilon)=\frac{r_\chi}{R_{\rm AdS}}\frac{\nu+i}{\bar{n}}\mathcal{F}'_n(\nu,\epsilon). \tag{A.6}$$

We can now plug these solutions into the boundary action to obtain the retarded R-current correlators. Following identical steps for the normalizable (in time) modes, we have

$$\mathcal{F}^{\rm N\prime}_n(\epsilon)=\frac{1}{4}\bar{n}^2\mathcal{F}^{\rm N0}_n\left(2\gamma_E+\ln\epsilon+\psi\left(1+\frac{i}{2}\bar{n}\right)+\psi\left(1-\frac{i}{2}\bar{n}\right)\right). \tag{A.7}$$

The induced boundary action for bulk Maxwell fields has the form

$$\begin{aligned}S\big|_{z=\epsilon}=&\frac{4\pi}{g^2_{\rm SG}}\sum_n\frac{1}{2\pi}\times\\ &\left(\int_{-\infty}^{\infty}\frac{d\nu}{2\pi}\left(r_\chi\mathcal{F}^0_{-n}(-\nu)\ \mathcal{F}'_n(\nu)\big|_{z=\epsilon}-\frac{R^2_{\rm AdS}}{r_\chi}\,\mathcal{G}^0_{-n}(-\nu)\ \mathcal{G}'_n(\nu)\big|_{z=\epsilon}\right)+r_\chi\mathcal{F}^{\rm N0}_{-n}\mathcal{F}^{\rm N\prime}_n\big|_{z=\epsilon}\right),\end{aligned} \tag{A.8}$$

JHEP04(2009)063

where $g^2_{\rm SG} = 16\pi^2 R_{\rm AdS}/N^2$. The complete real time retarded correlation functions for the R-currents, can now be accessed readily. First we define the boundary values of our gauge fields as

$$A_{\chi,\tau}(\epsilon,\tau,\chi) \equiv \sum_n \frac{e^{in\chi}}{2\pi} A^n_{\chi,\tau}(\tau)\,, \tag{A.9}$$

so that

$$\mathcal{G}^0_n(-\nu) = \int_{-\infty}^{\infty} A^n_\chi(\tau)\,\mathcal{T}_\chi(\nu,\tau)\cosh^2\tau. \tag{A.10}$$

and similarly

$$\mathcal{F}^0_n(-\nu) = \int_{-\infty}^{\infty} A^n_\tau(\tau)\,\mathcal{T}_\tau(\nu,\tau)\cosh^2\tau\,, \qquad \mathcal{F}^{\rm N0}_n = \int_{-\infty}^{\infty} A^n_\tau(\tau)\,\mathcal{T}^{\rm N}_\tau(\tau)\cosh^2\tau\,. \tag{A.11}$$

Putting these ingredients together, we find that the boundary action is

$$\begin{aligned} S\big|_{z=\epsilon} = {} & \frac{N^2}{4\pi R_{\rm AdS}} \sum_n \frac{1}{2\pi}\int_{-\infty}^{\infty} d\tau\,\cosh^2\tau \int_{-\infty}^{\infty} d\tau'\,\cosh^2\tau' \\ & \left[\int_{-\infty}^{\infty}\frac{d\nu}{2\pi}\left(2\gamma_E + \ln\epsilon + \psi\left(\frac{1}{2}+\frac{i}{2}(\bar n-\nu)\right)+\psi\left(\frac{1}{2}-\frac{i}{2}(\bar n+\nu)\right)\right)\times\right. \\ & \times\left(A^{-n}_\tau(\tau)A^n_\tau(\tau')\,\frac{\bar n^2}{4}\,r_\chi\;\mathcal{T}_\tau(\nu,\tau)\mathcal{T}_\tau(-\nu,\tau') \;-\; A^{-n}_\tau(\tau)A^n_\chi(\tau')\,R_{\rm AdS}\frac{\bar n}{4}(\nu-i)\times\right. \\ & \times\mathcal{T}_\tau(\nu,\tau)\mathcal{T}_\chi(-\nu,\tau') \;-\; A^{-n}_\chi(\tau)A^n_\tau(\tau')\,R_{\rm AdS}\frac{\bar n}{4}(\nu+i)\,\mathcal{T}_\chi(\nu,\tau)\mathcal{T}_\tau(-\nu,\tau') + \\ & \left.+A^{-n}_\chi(\tau)A^n_\chi(\tau')\frac{R^2_{\rm AdS}}{r_\chi}\frac{1}{4}(\nu^2+1)\mathcal{T}_\chi(\nu,\tau)\mathcal{T}_\chi(-\nu,\tau')\right) + r_\chi A^{-n}_\tau(\tau)A^n_\tau(\tau')\times \\ & \left.\times\frac{\bar n^2}{4}\mathcal{T}^{\rm N}(\tau)\mathcal{T}^{\rm N}(\tau')\left(2\gamma_E+\ln\epsilon+\psi\left(1+\frac{i}{2}\bar n\right)+\psi\left(1-\frac{i}{2}\bar n\right)\right)\right]. \end{aligned} \tag{A.12}$$

A.2 Nonzero momentum along the spatial slices of dS_3

Below we fill in the steps in the derivation of the boundary action for the Maxwell fields in the bulk. The asymptotic form of the radial dependence of the bulk potential $\mathcal{F}'_\ell$, can be determined from (3.72)

$$F_\ell\big|_{z\to 0} = C_\ell(\nu)\,(C_1(\nu) + C_2(\nu)\;\ln z)\,, \tag{A.13}$$

where

$$C_1 = -\frac{2\gamma_E + \psi(1-\frac{i\nu}{2}) + \psi(-\frac{i\nu}{2})}{\Gamma(1-\frac{i\nu}{2})\Gamma(-\frac{i\nu}{2})}, \tag{A.14a}$$

$$C_2 = -\frac{1}{\Gamma(1-\frac{i\nu}{2})\Gamma(-\frac{i\nu}{2})}. \tag{A.14b}$$

We can solve for C_ℓ in terms of the boundary values of the gauge potentials, using the bulk equation of motion (3.65b) for $\mathcal{F}'_\ell$ near the boundary which yields

$$4\int_{-\infty}^{\infty}\frac{d\nu}{2\pi}\,\Gamma(1+i\nu)P_\ell^{-i\nu}(\tanh\tau)\;\; C_\ell(\nu)\,C_2(\nu) = \ell(\ell+1)\left(\mathcal{F}^0_\ell(\tau) - \partial_\tau\mathcal{G}^0_\ell(\tau)\right). \tag{A.15}$$

JHEP04(2009)063

Note that the other equation of motion (3.65a) for $\mathcal{G}'_\ell$, just yields the time derivative of this condition, so that we have only one equation to determine the coefficient C_ℓ. This equation can be solved if we recall that the associated Legendre functions are mutually orthogonal[3]

$$\int_{-\infty}^{\infty} d\tau\ P_\ell^{i\nu}(\tanh\tau) P_\ell^{-i\nu'}(\tanh\tau) = \frac{\delta(\nu-\nu')}{\Gamma(1-i\nu)\Gamma(1+i\nu)}. \tag{A.16}$$

Thus, we have

$$C_\ell = \frac{\ell(\ell+1)}{4C_2}\Gamma(1-i\nu)\int_{-\infty}^{\infty} d\tau' \left(\mathcal{F}_\ell^0(\tau') - \partial_{\tau'}\mathcal{G}_\ell^0(\tau')\right)\ P_\ell^{i\nu}(\tanh\tau') \tag{A.17}$$

from which we obtain the solution

$$\begin{aligned}\cosh^2\tau\ \mathcal{F}'_\ell(\epsilon,\tau) = &\ \frac{\ell(\ell+1)}{4}\int_{-\infty}^{\infty} d\tau' \left(\mathcal{F}_\ell^0(\tau') - \partial_{\tau'}\mathcal{G}_\ell^0(\tau')\right) \\ &\left[\int_{-\infty}^{\infty}\frac{d\nu}{2\pi}\frac{\pi\nu}{\sinh\pi\nu}\ P_\ell^{-i\nu}(\tanh\tau)P_\ell^{i\nu}(\tanh\tau')\ \left(\ln\epsilon+2\gamma_E+\psi\left(-\frac{i\nu}{2}\right)+\psi\left(1-\frac{i\nu}{2}\right)\right)\right. \\ &\left. + \sum_{m=1}^{\ell} m\frac{(\ell-m)!}{(\ell+m)!}\ P_\ell^m(\tanh\tau)P_\ell^m(\tanh\tau')\left(\ln\epsilon+2\gamma_E+\psi\left(\frac{m}{2}\right)+\psi\left(1+\frac{m}{2}\right)\right)\right].\end{aligned} \tag{A.18}$$

Plugging these back into the expression for the boundary action (3.75), we obtain the generating functional for two point correlators of R-currents.

B WKB matching conditions

We explain below the matching conditions at the turning point(s) of the WKB potential for the Schrödinger equation (4.9a) in the AdS bubble of nothing background.

B.1 WKB matching conditions for $\nu > \tilde{r}_h$

Near the turning point $u = u_c$ corresponding to $\rho = \sqrt{1+\nu^2}$, since we are well away from any extrema, we can assume that

$$\mathcal{V}(\nu, u) = \kappa(u_c - u) + \dots, \qquad u \to u_c. \tag{B.1}$$

In this region where the potential is basically linear, the exact solution in terms of Airy functions is

$$\Psi\big|_{u\to u_c} = A_+\ \frac{2\sqrt{\pi}}{\kappa^{1/6}}\ \mathrm{Ai}\left(\kappa^{1/3}(u_c-u)\right) + A_-\ \frac{\sqrt{\pi}}{\kappa^{1/6}}\ \mathrm{Bi}\left(\kappa^{1/3}(u_c-u)\right). \tag{B.2}$$

The normalizations and constants of integration have been chosen carefully so that the exact solution near the turning point, in terms of Airy functions, matches the WKB solution (4.12) in Region I ($u < u_c$) away from the turning point. Now, we can continue the

[3] The orthogonality of these functions for purely imaginary order follows from the fact that they are eigenfunctions of the Schrödinger equation in the sech^2 potential, $\left(-\frac{d^2}{d\tau^2} - \ell(\ell+1)/\cosh^2\tau\right) P_\ell^{i\nu}(\tanh\tau) = \nu^2 P_\ell^{i\nu}(\tanh\tau)$. In particular for $\nu \in \mathbb{R}$, these are scattering states and are delta-function normalizable, and the eigenfunctions corresponding to two different eigenvalues are orthogonal as usual.

JHEP04(2009)063

solution (B.2) into Region II ($u > u_c$). For $u > u_c$, where the WKB solution (4.16) should be valid, the Airy functions have the asymptotic form

$$\Psi\big|_{u>u_c} \approx 2A_+ \frac{\sin\left(\frac{2}{3}\sqrt{\kappa}(u-u_c)^{3/2}+\frac{\pi}{4}\right)}{\kappa^{1/4}(u-u_c)^{1/4}} + A_- \frac{\cos\left(\frac{2}{3}\sqrt{\kappa}(u-u_c)^{3/2}+\frac{\pi}{4}\right)}{\kappa^{1/4}(u-u_c)^{1/4}}. \tag{B.3}$$

Comparison with (4.16) near the turning point then implies

$$B_+ = e^{i\frac{\pi}{4}}\left(\frac{1}{2}A_- - iA_+\right); \quad B_- = e^{-i\frac{\pi}{4}}\left(\frac{1}{2}A_- + iA_+\right). \tag{B.4}$$

There is yet another condition that emergies from the behaviour of the solutions near the second "turning point", $\rho \to \sqrt{1+\tilde{r}_h^2}$ or $u \to \infty$ where the space ends. In this region we have

$$\frac{du}{d\rho}\Big|_{\rho\to\sqrt{1+\tilde{r}_h^2}} \approx -\frac{\sqrt{1+\tilde{r}_h^2}}{2(2\tilde{r}_h^2+1)(\rho-\sqrt{1+\tilde{r}_h^2})} \tag{B.5}$$

so that

$$\rho - \sqrt{1+\tilde{r}_h^2} \;\approx\; 2\sqrt{1+\tilde{r}_h^2}\exp\left(-2\frac{(1+2\tilde{r}_h^2)}{\sqrt{1+\tilde{r}_h^2}}\,u + \frac{\tilde{r}_h}{\sqrt{1+\tilde{r}_h^2}}\cot^{-1}\left(\frac{\sqrt{1+\tilde{r}_h^2}}{\tilde{r}_h}\right)\right). \tag{B.6}$$

It follows then that, as a function of u, the high frequency potential decays exponentially,

$$\mathcal{V}(\nu,u)\big|_{u\to\infty} \approx (MR)^2\left(1-\frac{\nu^2}{\tilde{r}_h^2}\right)\exp\left(-2\frac{(1+2\tilde{r}_h^2)}{\sqrt{1+\tilde{r}_h^2}}\,u + \text{constants}\right). \tag{B.7}$$

Note that for $\nu > \tilde{r}_h$, the potential approaches zero from below. Let us define constants A and B, in terms of which the potential is simply

$$\tilde{V}_0(\nu,u)\big|_{u\to\infty} \approx -Ae^{-Bu}, \tag{B.8}$$

where A and B can be read off easily from the expressions above. The Schrödinger equation with an exponentially decaying potential is solved exactly by Bessel functions:

$$-\Psi''(u) - Ae^{-Bu}\Psi(u) = 0,$$
$$\Psi = C_1\, J_0\left(2\frac{\sqrt{A}}{B}\,e^{-Bu/2}\right) + C_2\, Y_0\left(2\frac{\sqrt{A}}{B}\,e^{-Bu/2}\right). \tag{B.9a}$$

Recall that we are looking for a zero energy eigenfunction of the Schrödinger problem. This means that for a potential that vanishes at infinity, the corresponding (normalizable) wavefunction can only be zero. This is an important difference to the black hole case where the wave functions are infalling plane waves at the horizon. Requiring that the wave function Ψ vanish or approach a constant as $u \to \infty$ then eliminates the term proportional to Y_0. Hence, in the exponentially decaying region

$$\Psi(u) \propto J_0\left(2\frac{\sqrt{A}}{B}\,e^{-Bu/2}\right). \tag{B.10}$$

JHEP04(2009)063

The WKB approximation should match onto the Bessel function for large values of the argument of the Bessel function. Using the standard asymptotic expansion for Bessel functions

$$J_0(x)\big|_{x\gg 1} \simeq \frac{\cos(x)}{\sqrt{\pi x}} + \frac{\sin(x)}{\sqrt{\pi x}}. \tag{B.11}$$

From this we can deduce a relationship between the constants B_+ and B_- in (4.16). To make this precise we define the integral

$$\mathcal{S}_{\rm II}(u) = \int_\infty^u \sqrt{|\mathcal{V}(\nu,u)|}\, du. = -MR \int_{\tilde r_h}^{\rho^2-1} dx \sqrt{\frac{x^2-\nu^2}{(x^2-\tilde r_h^2)(x^2+1+\tilde r_h^2)}} \tag{B.12}$$

where

$$\begin{aligned}\mathcal{S}_{\rm II}(u(\rho)) =& i\,\frac{MR}{\sqrt{1+2\tilde r_h^2}}\Bigg[\nu\Bigg(F\Bigg(\sin^{-1}\sqrt{\frac{1}{a}\frac{\rho^2+\tilde r_h^2}{\rho^2-1}},\ k\Bigg) - \frac{1}{\sqrt{k}}\,K\Big(\frac{1}{k}\Big)\Bigg)+\\ &+\frac{1}{\nu}(1+\tilde r_h^2)\Bigg(\Pi\Bigg(a;\ \sin^{-1}\sqrt{\frac{1}{a}\frac{\rho^2+\tilde r_h^2}{\rho^2-1}}\,\Big|\,k\Bigg) - \frac{1}{\sqrt{k}}\,\Pi\Big(b\Big|\frac{1}{k}\Big)\Bigg)\Bigg],\\ a =& \frac{\nu^2+1+\tilde r_h^2}{\nu^2}\ ; \qquad b = \frac{1+2\tilde r_h^2}{\tilde r_h^2}\ ; \qquad k = \frac{a}{b}.\end{aligned} \tag{B.13}$$

Then the WKB solution in Region II is

$$\Psi_{\rm WKB} = \frac{1}{|\mathcal{V}|^{1/4}}\left(B_+\, e^{i\mathcal{S}_{\rm II}(u)-i\mathcal{S}_{\rm II}(u_c)} + B_- e^{-i\mathcal{S}_{\rm II}(u)+i\mathcal{S}_{\rm II}(u_c)}\right). \tag{B.14}$$

For large u,

$$\mathcal{S}_{\rm II}(u)\big|_{u\gg 1} \approx \int_\infty^u \sqrt{A}e^{-Bu/2} = -2\frac{\sqrt{A}}{B}\, e^{-Bu/2}. \tag{B.15}$$

Using this result and comparing (B.14) to the asymptotics of the Bessel function (B.11), we find

$$\frac{B_+}{B_-} = \ ie^{2i\,\mathcal{S}_{\rm II}(u_c)}. \tag{B.16}$$

The final ingredient consists in determining A_+ and A_-. To this end we first define

$$\mathcal{S}_I(u) = \int^u \sqrt{\mathcal{V}(\nu,u)}\, du, \tag{B.17}$$

which then gives us

$$\begin{aligned}\mathcal{S}_I(u(\rho)) =& \frac{MR}{\sqrt{1+2\tilde r_h^2}}\Bigg[\nu F\Bigg(\sin^{-1}\left(\sqrt{\frac{1}{a}\frac{\rho^2+\tilde r_h^2}{\rho^2-1}}\right),\ k\Bigg)\\ &+\frac{1}{\nu}(1+\tilde r_h^2)\,\Pi\Bigg(a;\sin^{-1}\left(\sqrt{\frac{1}{a}\frac{\rho^2+\tilde r_h^2}{\rho^2-1}}\right)\Big|\,k\Bigg)\Bigg],\\ a =& \frac{\nu^2+1+\tilde r_h^2}{\nu^2}\ ; \qquad b = \frac{1+2\tilde r_h^2}{\tilde r_h^2}\ ; \qquad k = \frac{a}{b}.\end{aligned}$$

Near the boundary $u \to 0$ or equivalently $\rho \to \infty$, we find

$$\begin{aligned}\Psi_{\rm WKB} \approx A_- \frac{1}{\sqrt{MR}}\, \rho^{MR-\frac{1}{2}}\, e^{i\pi MR/2}\, \left(\frac{4}{1+\tilde{r}_h^2}\right)^{MR/4}\, \nu^{-MR/2}\times \\ \exp\left[\frac{MR}{\sqrt{1+2\tilde{r}_h^2}}\, \left(\nu(F\left(\csc^{-1}\sqrt{a},\ k\right) - K(k)) - \frac{1}{\nu}(1+\tilde{r}_h^2)\, \Pi(a|k)\right)\right] \\ +\ A_+ \frac{1}{\sqrt{MR}}\, \rho^{-MR-\frac{1}{2}}\, e^{-i\pi MR/2}\, \left(\frac{4}{1+\tilde{r}_h^2}\right)^{-MR/4}\, \nu^{MR/2}\times \\ \exp\left[-\frac{MR}{\sqrt{1+2\tilde{r}_h^2}}\, \left(\nu(F\left(\csc^{-1}\sqrt{a},\ k\right) - K(k)) - \frac{1}{\nu}(1+\tilde{r}_h^2)\, \Pi(a|k)\right)\right].\end{aligned} \tag{B.18}$$

Combining (B.4) and (B.16) we obtain

$$A_+ = -A_- \frac{1}{2}\, \tan\left(\mathcal{S}_{\rm II}(u_c)\right). \tag{B.19}$$

B.2 WKB matching for $|\nu| < \tilde{r}_h$

When $|\nu| < \tilde{r}_h$, the potential energy $\mathcal{V}(\nu, u)$ is a monotonic function of u which exponentially vanishes as $u \to \infty$. Now, the potential has effectively only one turning point and the wave function has no region where it propagates. The WKB solution (4.12) in Region I should smoothly match onto the exact solution of

$$-\psi''(u) + Ae^{-Bu}\psi(u) = 0\,, \qquad A, B > 0. \tag{B.20}$$

The solutions to these are the modified Bessel's functions. Enforcing regular behaviour as $u \to \infty$ picks out

$$\psi(u) \propto I_0\left(2\frac{\sqrt{A}}{B}e^{-Bu/2}\right). \tag{B.21}$$

The WKB approximation for $I_0(x)$ is valid when $x \gg 1$,

$$I_0(x)\big|_{x\gg 1} \simeq \frac{1}{2\sqrt{2\pi x}}\left(e^x + ie^{-x}\right). \tag{B.22}$$

We write the WKB solution to the wave equation in the bubble of nothing background as

$$\Psi_{\rm WKB}(\nu, u) = A_+ \frac{1}{\mathcal{V}^{1/4}} \exp\left(\int_\infty^u \sqrt{\mathcal{V}}du\right) + A_- \frac{1}{\mathcal{V}^{1/4}} \exp\left(-\int_\infty^u \sqrt{\mathcal{V}}du\right). \tag{B.23}$$

Comparison with the modified Bessel function implies

$$A_+ = iA_-. \tag{B.24}$$

Near the boundary $u \to 0$, which is equivalent to $\rho \to \infty$, we have

$$\Psi_{\rm WKB} \approx A_- \frac{1}{\sqrt{MR}}\, \rho^{MR-\frac{1}{2}}\, e^{i\pi MR/2} \left(\frac{4}{1+\tilde{r}_h^2}\right)^{MR/4} \nu^{-MR/2} \times$$
$$\exp\left[\frac{MR}{\sqrt{1+2\tilde{r}_h^2}} \left(\nu(F\left(\csc^{-1}\sqrt{a},\ k\right) - \frac{1}{\sqrt{k}} K\left(\frac{1}{k}\right) - \frac{1}{\nu}(1+\tilde{r}_h^2)\, \frac{1}{\sqrt{k}} \Pi\left(a\middle|\frac{1}{k}\right)\right)\right]$$
$$+\ A_+ \frac{1}{\sqrt{MR}}\, \rho^{-MR-\frac{1}{2}}\, e^{-i\pi MR/2} \left(\frac{4}{1+\tilde{r}_h^2}\right)^{-MR/4} \nu^{MR/2} \times$$
$$\exp\left[-\frac{MR}{\sqrt{1+2\tilde{r}_h^2}} \left(\nu(F\left(\csc^{-1}\sqrt{a},\ k\right) - \frac{1}{\sqrt{k}} K\left(\frac{1}{k}\right) - \frac{1}{\nu}(1+\tilde{r}_h^2)\, \frac{1}{\sqrt{k}} \Pi\left(a\middle|\frac{1}{k}\right)\right)\right]. \tag{B.25}$$

References

[1] J.M. Maldacena, *The large-N limit of superconformal field theories and supergravity*, *Adv. Theor. Math. Phys.* **2** (1998) 231 [*Int. J. Theor. Phys.* **38** (1999) 1113] [hep-th/9711200] [SPIRES].

[2] O. Aharony, S.S. Gubser, J.M. Maldacena, H. Ooguri and Y. Oz, *Large-N field theories, string theory and gravity*, *Phys. Rept.* **323** (2000) 183 [hep-th/9905111] [SPIRES].

[3] D. Birmingham and M. Rinaldi, *Bubbles in Anti-de Sitter space*, *Phys. Lett.* **B 544** (2002) 316 [hep-th/0205246] [SPIRES].

[4] V. Balasubramanian and S.F. Ross, *The dual of nothing*, *Phys. Rev.* **D 66** (2002) 086002 [hep-th/0205290] [SPIRES].

[5] R.-G. Cai, *Constant curvature black hole and dual field theory*, *Phys. Lett.* **B 544** (2002) 176 [hep-th/0206223] [SPIRES].

[6] S.F. Ross and G. Titchener, *Time-dependent spacetimes in AdS/CFT: bubble and black hole*, *JHEP* **02** (2005) 021 [hep-th/0411128] [SPIRES].

[7] V. Balasubramanian, K. Larjo and J. Simon, *Much ado about nothing*, *Class. Quant. Grav.* **22** (2005) 4149 [hep-th/0502111] [SPIRES].

[8] O. Aharony, M. Fabinger, G.T. Horowitz and E. Silverstein, *Clean time-dependent string backgrounds from bubble baths*, *JHEP* **07** (2002) 007 [hep-th/0204158] [SPIRES].

[9] E. Witten, *Instability of the Kaluza-Klein vacuum*, *Nucl. Phys.* **B 195** (1982) 481 [SPIRES].

[10] R.C. Myers and M.J. Perry, *Black holes in higher dimensional space-times*, *Ann. Phys.* **172** (1986) 304 [SPIRES].

[11] F. Dowker, J.P. Gauntlett, G.W. Gibbons and G.T. Horowitz, *The decay of magnetic fields in Kaluza-Klein theory*, *Phys. Rev.* **D 52** (1995) 6929 [hep-th/9507143] [SPIRES].

[12] D. Astefanesei and G.C. Jones, *S-branes and (anti-)bubbles in (A)dS space*, *JHEP* **06** (2005) 037 [hep-th/0502162] [SPIRES].

[13] R. Emparan, *AdS/CFT duals of topological black holes and the entropy of zero-energy states*, *JHEP* **06** (1999) 036 [hep-th/9906040] [SPIRES].

JHEP04(2009)063

[14] J. Alsup and G. Siopsis, *Low-lying quasinormal modes of topological AdS black holes and hydrodynamics*, *Phys. Rev.* **D 78** (2008) 086001 [arXiv:0805.0287] [SPIRES].

[15] G. Koutsoumbas, E. Papantonopoulos and G. Siopsis, *Discontinuities in scalar perturbations of topological black holes*, arXiv:0806.1452 [SPIRES].

[16] G. Koutsoumbas, E. Papantonopoulos and G. Siopsis, *Shear viscosity and Chern-Simons diffusion rate from hyperbolic horizons*, arXiv:0809.3388 [SPIRES].

[17] M. Bañados, *Constant curvature black holes*, *Phys. Rev.* **D 57** (1998) 1068 [gr-qc/9703040] [SPIRES].

[18] M. Bañados, A. Gomberoff and C. Martinez, *Anti-de Sitter space and black holes*, *Class. Quant. Grav.* **15** (1998) 3575 [hep-th/9805087] [SPIRES].

[19] M. Bañados, M. Henneaux, C. Teitelboim and J. Zanelli, *Geometry of the* $(2+1)$ *black hole*, *Phys. Rev.* **D 48** (1993) 1506 [gr-qc/9302012] [SPIRES].

[20] M. Bañados, C. Teitelboim and J. Zanelli, *The black hole in three-dimensional space-time*, *Phys. Rev. Lett.* **69** (1992) 1849 [hep-th/9204099] [SPIRES].

[21] S.W. Hawking and D.N. Page, *Thermodynamics of black holes in Anti-de Sitter space*, *Commun. Math. Phys.* **87** (1983) 577 [SPIRES].

[22] E. Witten, *Anti-de Sitter space and holography*, *Adv. Theor. Math. Phys.* **2** (1998) 253 [hep-th/9802150] [SPIRES].

[23] G.W. Gibbons and S.W. Hawking, *Cosmological event horizons, thermodynamics and particle creation*, *Phys. Rev.* **D 15** (1977) 2738 [SPIRES].

[24] C.P. Herzog and D.T. Son, *Schwinger-Keldysh propagators from AdS/CFT correspondence*, *JHEP* **03** (2003) 046 [hep-th/0212072] [SPIRES].

[25] K. Skenderis and B.C. van Rees, *Real-time gauge/gravity duality*, *Phys. Rev. Lett.* **101** (2008) 081601 [arXiv:0805.0150] [SPIRES].

[26] K. Skenderis and B.C. van Rees, *Real-time gauge/gravity duality: prescription, renormalization and examples*, arXiv:0812.2909 [SPIRES].

[27] D.T. Son and A.O. Starinets, *Minkowski-space correlators in AdS/CFT correspondence: recipe and applications*, *JHEP* **09** (2002) 042 [hep-th/0205051] [SPIRES].

[28] G. Policastro, D.T. Son and A.O. Starinets, *From AdS/CFT correspondence to hydrodynamics*, *JHEP* **09** (2002) 043 [hep-th/0205052] [SPIRES].

[29] D.T. Son and A.O. Starinets, *Viscosity, black holes and quantum field theory*, *Ann. Rev. Nucl. Part. Sci.* **57** (2007) 95 [arXiv:0704.0240] [SPIRES].

[30] G.T. Horowitz and E. Silverstein, *The inside story: quasilocal tachyons and black holes*, *Phys. Rev.* **D 73** (2006) 064016 [hep-th/0601032] [SPIRES].

[31] E. Mottola, *Particle creation in de Sitter space*, *Phys. Rev.* **D 31** (1985) 754 [SPIRES].

[32] N.D. Birrell and P.C.W. Davies, *Quantum fields in curved space*, Cambridge University Press, Cambridge U.K. (1982) [SPIRES].

[33] M. Spradlin, A. Strominger and A. Volovich, *Les Houches lectures on de Sitter space*, hep-th/0110007 [SPIRES].

[34] S.A. Hartnoll and S. Prem Kumar, *AdS black holes and thermal Yang-Mills correlators*, *JHEP* **12** (2005) 036 [hep-th/0508092] [SPIRES].

JHEP04(2009)063

[35] P. Kovtun, M. Ünsal and L.G. Yaffe, *Volume independence in large-N_c QCD-like gauge theories*, *JHEP* **06** (2007) 019 [hep-th/0702021] [SPIRES].

[36] M. Ünsal and L.G. Yaffe, *Center-stabilized Yang-Mills theory: confinement and large-N volume independence*, *Phys. Rev.* **D 78** (2008) 065035 [arXiv:0803.0344] [SPIRES].

[37] D. Boyanovsky, R. Holman and S. Prem Kumar, *Inflaton decay in de Sitter spacetime*, *Phys. Rev.* **D 56** (1997) 1958 [hep-ph/9606208] [SPIRES].

[38] L. Fidkowski, V. Hubeny, M. Kleban and S. Shenker, *The black hole singularity in AdS/CFT*, *JHEP* **02** (2004) 014 [hep-th/0306170] [SPIRES].

[39] G. Festuccia and H. Liu, *Excursions beyond the horizon: black hole singularities in Yang-Mills theories. I*, *JHEP* **04** (2006) 044 [hep-th/0506202] [SPIRES].

[40] C. Csáki, H. Ooguri, Y. Oz and J. Terning, *Glueball mass spectrum from supergravity*, *JHEP* **01** (1999) 017 [hep-th/9806021] [SPIRES].

[41] See http://functions.wolfram.com/.

[42] M. Abramowitz and I.A. Stegun, *Handbook of mathematical functions with formulas, graphs, and mathematical tables*, Dover Publications, New York U.S.A. (1964).

JHEP04(2009)063